1-1-2013

Gelation Characteristics and Osteogenic Differentiation of Stromal Cells In Inert Hydrolytically Degradable Micellar Polyethylene Glycol Hydrogels

Danial Barati
University of South Carolina

Gelation Characteristics and Osteogenic Differentiation of Stromal Cells in Inert Hydrolytically Degradable Micellar Polyethylene Glycol Hydrogels

by

Danial barati

Bachelor of Science

University of Tehran, 2009

Submitted in Partial Fulfillment of the Requirements

For the Degree of Master of Science in

Chemical Engineering

College of Engineering and Computing

University of South Carolina

2013

Accepted by:

Esmaiel Jabbari, Major Professor

Jay Blanchette, Committee Member

Tarek Shazly, Committee Member

Lacy Ford, Vice Provost and Dean of Graduate Studies

Acknowledgments

First of all, I am deeply and sincerely grateful to my advisor, Professor Dr. Esmaiel Jabbari in the Chemical and Biomedical Engineering Department at the University of South Carolina. He helped me to broaden my knowledge and guided me throughout the whole research project. I also want to thank to my research group members Dr. Xuezhong He Dr. Angel E Mercado for their useful suggestions during my research. I also want to thank Chemical Engineering secretary Marcia Rowen for her help during my study. I would like to express my sincere thanks to all of them.

Also, this work was supported by research grants to E. Jabbari from the National Science Foundation under grant Nos. CBET0756394, CBET0931998, and DMR1049381, the National Institutes of Health under Grant No. DE19180, and the Arbeitsgemeinschaft Fur Osteosynthesefragen (AO) Foundation under Grant No. C10-44J.

I would also want to thank all my family members for encouraging and supporting me to get my master degree thousands miles away from my country.

Abstract

The use of polyethylene glycol (PEG) hydrogels in tissue engineering is limited by their persistence in the site of regeneration. In an attempt to produce degradable PEG-based hydrogels while preserving the unique properties of PEG, linear (LPELA) and star (SPELA) poly(ethylene glycol-co-lactide) acrylate, star (SPEDA) poly(ethylene glycol-co-dioxanone), star (SPEGA) poly(ethylene glycol-co-glycolide) acrylate as the least hydrophobic and (SPECA) poly(ethylene glycol-co-caprolactone) as the most hydrophobic macromonomers with short hydrophobic segments were synthesized. The hydrogels were characterized with respect to gelation time, modulus, water content, sol fraction, degradation, and osteogenic differentiation of encapsulated marrow stromal cells (MSCs). Chain extension of PEG with short hydrpphobic segments resulted in micelle formation for all types of macromonomers. Due to micelle formation, there was a significant decrease in gelation time of SPEXA precursor solutions with degradable hydrophobic chain extension for all types. The star SPELA hydrogel had higher modulus, lower water content, and lower sol fraction than the linear LPELA. The shear modulus of star SPELA hydrogel was 2.2 fold higher than LPELA while the sol fraction of SPELA hydrogel was 5 fold lower than LPELA. The degradation of SPELA hydrogels depended strongly on the number of lactide monomers per macromonomer (nL) and showed a biphasic behavior. For example, as nL increased from zero to 3.4, 6.4, 11.6, and 14.8, mass loss increased from 7 to 37, 80, 100%, and then deceased to 87%, respectively, after

6 weeks of incubation. SPEXA gels chain extended with the least hydrophobic glycolide showed the highest mechanical strength and completely degraded within days, lactide within weeks, p-dioxanone and ε-caprolactone degraded within months. The wide range of degradation rates observed for SPEXA gels can be explained by large differences in equilibrium water content of the micelles for different HA monomers. MSCs encapsulated in SPELA hydrogels, with or without supplementing with bone morphogenetic protein-2 (BMP2), expressed osteogenic markers Dlx5, Runx2, osteopontin, and osteocalcin and formed a mineralized matrix. The expression of osteogenic markers and extent of minerlization was significantly higher in the presence of BMP2. Results demonstrate that hydrolytically degradable PEG-based hydrogels are potentially useful as a delivery matrix for stem cells in regenerative medicine.

Table of Contents

List of Figures

1. Background

1.1 Introduction

Man has always suffered from ailments and diseases of both the body and the mind. However dedicated efforts from scientists all over the world are making it possible to treat, prevent and eradicate many of these diseases that plague man. One of the fields of research that has made a great progress in the past few decades is the treatment of diseases via biomolecules such as drugs, proteins etc. [1,16]. Initially these could only be applied in limited manner, due to limitations of drug delivery through harmful environments in the body. Therefore, limited mobility reduced the effectiveness of administered drugs. Further improvement came with the development of biomaterial carriers which could be encapsulated, or immobilized with drugs, allowing the drug to be safely delivered to the required site without harm [1, 23]. These carriers allowed for the release of drug in sites which were previously inaccessible. The nature of these carriers was evolved over the years from ceramics, to natural, to synthetic materials. Different criteria such as integrity, biocompatibility and flexibility were considered, and led to the use of hydrophilic three dimensional network structures as carrier materials. These are a class of materials known as *Hydrogels*. The most important characteristic of these three dimensional polymer matrices is the capability of soaking up large amounts of water, and biological fluids without dissolving. This property of hydrogels is the reason behind its

wide range of applications from food additives to pharmaceuticals and clinical applications [10, 16].

Synthetic hydrogels prepared from a various types of monomers have attracted many attentions especially in tissue-engineering scaffolds, as carriers for implantable devices, and drug delivery devices. Synthetic hydrogels provide an effective and controlled way in which to use protein and peptide based drugs for treatment of a number of diseases. A successful drug delivery device relies not only on competent network design, but also on accurate mathematical modeling of drug release profiles. Hydrogels have ordered polymer networks, with well-defined chemistries yielding well-defined physicochemical properties and easily reproducible drug release profiles. Hydrogels have thus become a premier material used for drug delivery formulations and biomedical implants, due to its biocompatibility, network structure, and molecular stability of the incorporated bioactive agent.

1.2 Properties of Hydrogels

Hydrogels are water swollen polymer network, with a tendency to absorb water when placed in aqueous environment. This ability to swell, under biological conditions, makes it an ideal material for use in drug delivery and immobilization of proteins, peptides, and other biological compounds. Due to their high water content, these gels mimic natural living tissue more effective than any other type of synthetic biomaterial [1, 15]. These networks, have a three dimensional structure, crosslinked together either physically (entanglements, crystallites), or chemically (tie-points, junctions). This insoluble crosslinked structure allows immobilization of active agents, biomolecules effectively, and allows for its release in well-defined specific trend.

It is crucial that the carrier gel matrix keep up the physical and mechanical integrity. Mechanical stability of the gel is, therefore, an important consideration when designing a therapeutic system. For example, drugs and other biomolecules must be protected from the harmful environments in the body such as, extreme pH environment before it is released at the required site. For this reason, the carrier matrices must be able to preserve its physical integrity and mechanical strength in order to prove an effective biomaterial. The strength of the material can be controlled by incorporating crosslinking agents, comonomers, and changing the degree of crosslinking. There is however an optimum degree of crosslinking, because a higher degree of crosslinking may lead to brittleness and less elasticity. Elasticity of the gel is important to give flexibility to the crosslinked chains, to facilitate movement of incorporated bioactive agent. Thus a compromise between mechanical strength and flexibility is necessary for appropriate use of these materials.

Moreover, it is important for synthetic materials, such as hydrogels, to be biocompatible and nontoxic in order for it to be applicable in biomedical purposes. All polymers used for biomedical application must pass a cytotoxicity and in-vivo toxicity tests. Most toxicity problems associated with hydrogels come from unreacted monomers, oligomers and initiators that leach out during application. To reduce chances of toxic effects, the use of initiators is being eliminated, with the advent of gamma irradiation as polymerization technique. Steps are also taken to eliminate contaminants from hydrogels, by repeated sterilization and treatment [8, 14]. Also, kinetics of polymerization has been studied, so as to achieve higher conversion rates, and avoid unreacted monomers and side products.

1.3 Classification of Hydrogels

Hydrogels can be categorized into natural or synthetic groups. Hydrogels from natural sources can be derived from polymers such as collagen, hyaluronic acid (HA), fibrin alginate, agarose, and chitosan. Depending on their origin and composition, various natural polymers have specific utilities and properties. Polymer networks can be synthesized using various chemical methods (e.g., photo- and thermal-initiated polymerization) [11, 31]. The polymer engineer can design and synthesize polymer networks with molecular-scale control over structure such as crosslinking density and with tailored properties, such as biodegradation, mechanical strength, and chemical and biological response to stimuli. Hydrogels can also be classified as neutral or ionic, based on the nature of side groups. In neutral hydrogels, the driving force for swelling is due to the water-polymer thermodynamic mixing contribution to the overall free energy, along with elastic polymer contribution [3, 18]. The swelling of ionic hydrogels is also affected by the ionic interactions between charged polymers and free ions. Ionic hydrogels containing ionic groups, such as carboxylic acid, absorb larger amount of water due to their increased hydrophilicity such as poly (acrylic acid) and polyamines. Hydrogels can be classified based on the physical structure of the network as amorphous, semicrystalline, hydrogen bonded structures, supermolecular structures and hydrocolloidal aggregates [1, 21]. An important class of hydrogels is the stimuli responsive gels. These gels show swelling behavior dependent on their physical environment. These gels can swell, or deswell in response to variations of pH, temperature, ionic strength, and electromagnetic radiation.

1.4 Fabrication Methods of Hydrogels

One of the most frequently applications of hydrogels is controlled release of bioactive agents and for encapsulation of cells and biomolecules. In many of these cases the three dimensional structure of the hydrogels have to disintegrate into harmless non toxic products to ensure biocompatibility of the gel [1, 27]. The nature of the degradation products can be tailored by a suitable selection of the hydrogel building blocks. Considering this, various chemical and physical crosslinking methods can be used today for the design of biocompatible hydrogels. Chemically crosslinked gels have ionic or covalent bonds between polymer chains. Even though this leads to more mechanical stability, some of the crosslinking agents used can be toxic, and give unwanted reactions, thus rendering the hydrogel unsuitable for biological use. These adverse effects can be removed with the use of physically crosslinked gels. In physically crosslinked gels, dissolution is prevented by physical interactions between different polymer chains such as hydrophobic interactions. Both of these methods are used today for fabrication of synthetic hydrogels and are discussed in detail. In this project, the hydrogels were crossslinked via free radical polymerization under exposure of UV radiation, without the use of a crosslinking agent.

1.4.1 Chemically Crosslinked Gels

It was mentioned that chemically crosslinked hydrogels are mechanically quite stable because of the ionic and covalent bond which form these gels. However, the addition of crosslinking agent can adversely affect if the compound is toxic, which on liberation in the body becomes quite harmful. The various methods for chemical crosslinking are as follows:

- Crosslinking of Polymers: In this method chemically crosslinked gels are formed by radical polymerization of low molecular weight homopolymers, or copolymers in the presence of crosslinking agent. This reaction is mostly carried out in solution for biomedical applications. Since most hydrophilic polymers have enough hydroxyl groups, some agents such as aldehydes, maleic and oxalic acid, dimethylurea, diisocyanates etc that condense when organic hydroxyl groups are used as crosslinking agents. The solvent used for these reactions is usually water, but methanol, ethanol and benzyl alcohol have also been used. These solvents can be used only if after formation of network structure, the solvent can be exchanged with water [1, 37].
- Copolymerization reactions: Copolymerization reactions are used to produce polymer gels, Many hydrogels are produced in this fashion, for example poly (hydroxyalkyl methylacrylates). Initiators used in these reactions are radical and anionic initiators. Various initiators are used, such as Azobisisobutyronitrile (AIBN), benzoyl peroxide etc. Solvents can be added during the reaction to decrease the viscosity of the solution.

- Kinetic Mechanism: The whole crosslinking mechanism consists of four steps: initiation, propagation, crosslinking, and termination. Termination can occur by combination, disproportionation, and chain transfer to monomer. An example of a representative reaction scheme follows [1, 37]:

$$I \xrightarrow{k_d} 2A$$

$$A + M_1 \xrightarrow{k_{i1}} P_{1,0,0}$$

$$P_{p,q,r} + P_{x,y,z} \xrightarrow{k_{p12}} Q_{p,q,r+1} + P_{x,y-1,z+1}$$

$$P_{p,q,r} + P_{x,y,z} \xrightarrow{k_{tc11}} M_{p+x,q+y,r+z}$$

$$P_{p,q,r} + P_{x,y,z} \xrightarrow{k_{d111}} M_{p,q,r} + M_{x,y,z}$$

$$P_{p,q,r} + M_1 \xrightarrow{k_{f11}} M_{p,q,r} + P_{1,0,0}$$

$$P_{p,q,r} + P_{x,y,z} \xrightarrow{k_{f12}} M_{p,q,r} + P_{1,y-1,z+1} + Q_{0,0,1}$$

Where, I is the initiator, and A is a molecule with initiated radical. Here $P_{p\ ,q\ ,r}$ and $Q_{p\ ,q\ ,r}$ represent living polymer chains with monomethyacyl and dimethylacryl monomer terminal groups, respectively and $M_{p,q\ ,r}$ us dead polymer chain. The subscripts p, q, r are used to describe primary chain; they refer to monomethyacryl units, pendant methacryl groups, and cross-links per chain respectively.

- Crosslinking by High Energy Radiation: High energy radiation, such as gamma and electron beam radiation can be used to polymerize unsaturated compounds. Water soluble polymers derivatized with vinyl groups can be converted into hydrogels using high energy radiation. For example, PEG derivatized to PEGDA can form hydrogels once irradiated with UV radiations. Polymers without additional vinyl groups can also be crosslinked via radiation. On exposure to gamma or electron beam radiation, aqueous solutions of polymers form radicals on the polymer chains (e.g by the hemolytic scission of C-H bonds) [1, 38].

- Crosslinking Using Enzymes: Recently a new method was published using an enzyme to synthesize PEG-based hydrogels [1, 5]. A tetrahydroxy PEG was functionalized with addition of glutaminyl groups and networks were formed by addition of transglutaminase into solution of PEG and poly (lysine-cophenylalanine). This enzyme catalyzed reaction between γ-carboxamide group of PEG and the ε- amine group of lysine to obtain an amide linkage between polymers. The gel properties can be tailored by changing ratios of PEG and lysine.

1.4.2 Physically Crosslinked Hydrogels

Chemically crosslinked gels are followed by using a crosslinking agent, which can be toxic. This requires that the crosslinking agent be removed from gel, which can affect the gel mechanical strength. For these reasons, physically crosslinked gels are now coming into prominence. Different methods have been investigated exploring preparation of physically crosslinked gels. Below are mentioned some of the most widely used methods and their areas of application.

- Crosslinking by Ionic Interactions: An example of crosslinking by ionic interactions is crosslinking of Alginate. Alginate consists of glucuronic acid residues and mannuronic residues can be crosslinked by calcium ions. Crosslinking can be carried out at normal temperature and pH. These gels are used as matrix for encapsulation of cells and for release of proteins. Also, hydrogels made of Chitosan, as well as dextran based hydrogels, crosslinked with potassium ions are other gels synthesized with ionic interactions. In addition to anionic polymers being crosslinked with metallic ions, hydrogels can also be obtained by complexation of polyanions and polycations [1, 9].
- Crosslinking by Crystallization: Gel formation using this method is attributed to the formation of polymer crystallites which act as physical crosslinking sites in the network. The gel properties could be modified by varying polymer concentration, temperature, and freezing and thawing cycle times. These gels have been shown to be useful for drug release. An aqueous solution of PVA that undergoes a freeze-thaw process yields a strong highly elastic gel is an example of crosslinking by crystallization [1, 11].
- Crosslinking by Hydrogen Bonds: The hydrogen bonds are only formed when the carboxylic acid groups are protonated. This also implies that the swelling of gels is pH

dependent. Recently a hydrogel system was developed using the principle of DNA hybridization via hydrogen bonding. In this approach, oligodeoxyribonucleotides were coupled to a water soluble polymer. Poly(acrylic acid) and poly(methacrylic acid) form complexes with poly(ethylene glycol) by hydrogen bonding between the oxygen of the poly(ethylene glycol) and the carboxylic acid group of poly((meth)acrylic acid). Hydrogels were prepared by addition of a complementary oligodinucleotide (ODN) either conjugated to the same water soluble polymer or, in its free form, to an aqueous solution of the ODN derivatized water soluble copolymer.

- Crosslinking by Protein Interaction: Genetic Engineering has also been used for the fabrication of hydrogels. The major point of this method is that the sequence of peptides and, therefore its physical and chemical properties can be precisely tailored by the appropriate design of the genetic code in synthetic DNA sequences. Cappello and coworkers prepared sequential block copolymers containing a repetition of silk-like and elastine-like blocks, in which the insoluble silk-like segments are associated in the form of aligned hydrogen bonded beta strands or sheets. These hydrogels can also be used for drug delivery with drug release influenced by concentration, polymer composition, and temperature. Crosslinking by antigen-antibody interaction was also performed, in which an antigen (rabbit IgG) was grafted to chemically crosslinked polyarylaide in the presence of an additional crosslinker [1, 13].

1.5 Monomers Used for Fabrication of Hydrogels

Depending upon the application, hydrogel monomers are chosen according to their properties, ease of delivery or encapsulations, as well as cost and availability. The first synthesis of hydrogel was that of Wichterle and Lin [1, 17] using PHEMA (poly (hydroxyethyl methacrylate)) as the monomer. One of the most traditional monomers used for drug delivery of proteins is biodegradable PLGA (copolymer of lactic and glycolic acid). However these hydrophobic materials have a tendency to denature protein as well as cause inflammation due to degradation. These problems were overcome when researchers turned towards hydrophilic monomers. Monomers such as acrylic acid, polyethylene glycol, and methacrylic acid are all materials used in therapeutic applications. Scientists are today trying to synthesize macromers to suit specific applications. PNIPAAm (poly (Nisopropylacrylamide), PVA (polyvinyl alcohol) are all synthesized by new preparation techniques, for a variety of applications.

1.5.1 Polyethylene glycol (PEG)

It is known that hydrophilic monomers provide a distinct advantage in both fabrication and application of hydrogels. The premier material used today for both drug delivery, cell encapsulation and as adhesion promoters is Polyethylene glycol (PEG) hydrogels. PEG has many unique properties which make it an ideal choice [1, 22]. PEG and its “stealth “ properties , that is once its attached to certain formulations, it allows slow release of the formulation, thus enabling controlled release, as well as reduce uptake of harmful immunoglobins. This allows longer dosage and reduces immunogenicity of substances such as adenosine deaminase (ADA) and asparaginase. PEG is nontoxic, thus ideal for biological applications, and can be injected into the body without adverse

effects. It is also an FDA approved materials for use in humans. PEGylation is an important technique being developed for drug delivery, involves attachment of PEG to proteins and drugs, and has great potential for improving pharmokinetic and pharmodynamic properties of delivered drugs. Thus PEG has varied uses in the medical field, including drug delivery (e.g.; treatment of hepatitis C), laxatives, cell immobilization, (as adhesion promoters), biosensor materials, and encapsulation of islets of langerhans for treatment of diabetes. It is also used as carrier material for encapsulated cells for tissue engineering purposes. Thus PEG, with its biocompatibility, flexibility and stealth properties is an ideal material for use in pharmaceutical applications.

1.6 Applications of Hydrogels

Water- swollen crosslinked hydrogels have shown various applications in fields such as food additives, pharmaceutical as well as biomedicine. Natural and synthetic polymers are used for encapsulation of cells, as well as encapsulation of islets in a semipermeable membrane. Hydrogels have been used to prevent adhesions and prevent thrombosis after surgery, and as cell adhesion resistant surfaces. Microfabricated hydrogel arrays are also used for biosensing. Hydrogels now play an important role in tissue engineering scaffolds, iosensor and BioMEMS devices and drug carriers. Moreover, proteins, peptides, DNA based drugs can all be delivered via hydrogel carrier device. Biocompatibility, hydrophilicity and flexibility of hydrogels make it ideal for use as drug delivery matrix [1, 18].

Hydrogels show good compatibility with blood and other body fluids, thus are used as materials for contact lenses, burn wound dressings, membranes, and as coating applied to living surfaces. Natural and synthetic polymers have applications as wound dressings,

encapsulation of cells, and recently are being used in the new field of tissue engineering as matrices for repairing and regenerating a wide variety of tissues and organs. When parts, or whole tissues, organs fail, treatments include repair, replacement with a natural or synthetic substitute, or regeneration. Implants have been reasonably successful; however tissue engineering holds great promise for regeneration [1, 25].

The major class of biomaterials considered as implantable drug delivery systems are hydrogels. These hydrophilic networks are capable of absorbing great amounts of water while maintaining structural integrity [1.36]. Their structural similarity to the extracellular matrix makes it biocompatible. These synthetic polymers have generated wide interests and are now at the forefront of drug delivery research. In order to incorporate a preformed gel into the body, an opening must be created, with at least the same dimension as that of the gel. This leads to potential risk and discomfort to the patient. Thus focus has shifted to developing injectable materials with ability to form three dimensional matrices under physiological matrices. This in situ formation can be achieved through specific chemical crosslinking reactions. Gel structuring is triggered by environmental stimuli (pH, temperature, solvent exchange etc). The use of hydrogels allows not only delivery of drugs, but also controlled release, in the manner required by the pharmaceutical scientists. For example, drugs can be delivered only when needed, may be directed to specific site, and can be delivered at specific rates required by the body.

Hydrogels possess several properties that make them an ideal material for drug delivery. First, hydrogels can be tailored to respond to a number of stimuli. This enables sustained drug delivery corresponding to external stimuli such as pH or temperature.

These pH sensitive gels are useful in oral drug delivery as they can protect proteins in the digestive track. pH responsiveness is also useful for lysosomal escape during gene delivery. Second, Hydrogels can also be synthesized to exhibit bioadhesiveness to facilitate drug targeting, especially through mucus membranes, for non-invasive drug administration. Finally, Hydrogels also have a “stealth” characteristic in vivo circulation time of delivery device by evading the host immune response and decreasing phagocytic activity [1.23].

1.7 Network Structure of Hydrogels

The properties of the hydrogel which make it favorable for use in various pharmaceutical as well as medicinal purposes arise mostly from its crosslinked structure [38.50]. The crosslinked structure of the gel is determined by the nature of monomers, method of preparation, and nature of crosslinking agent. To understand the crosslinked structure of the gel, the most common approach used is the study of gel swelling. The swelling of the gel is studied and certain parameters of swelling are calculated [20.23]. Knowledge of the swelling characteristics of the gel is the first step in understanding the network structure of the gel and its capacity to function as a drug delivery carrier. Several theories have been proposed to explain the network structure of the gel, as well as the mechanism of swelling of gel. Some theories take into account the real network structure with defects, while others consider ideal network structure, due to its simplicity in analysis. In each of these cases, the hydrogel is exposed to a penetrant solvent and allowed to swell until equilibrium is reached [39.42]. Once the hydrogel is exposed to solvent, the gel swells, and the thermodynamically driven swelling force is

counterbalanced by the retractive force of the crosslinked structure, leading to an equilibrium state. This swollen state allows widening of the gap between the crosslinks and mesh size, thus facilitating the transfer of different solutes through the gel. The transfer of the solute is controlled by the swelling of the gel. Once this information is known, the gel can be manipulated by varying mesh size, and property of drug to enable diffusion of required drug in specific manner.

1.7.1 Characterzation of Crosslinked structure:

Hydrogels are actually cross linked three dimensional matrices, which can be formed by covalent, ionic, and, in some cases, by Van der waals and hydrogen bonds. The network structure of the hydrogel depends on its constituent monomers, the method of preparation and method of crosslinking. Most hydrogels used for biomedical applications are noncrystalline. These networks contain localized ordered structures or nonhomogenous structures, unlike the common Flory picture of a randomly crosslinked mass of molecular chains. Characterization of the hydrogel network structure is quite complicated because of the many types of possible networks, including regular, irregular, loosely crosslinked, highly crosslinked and imperfect networks. For the purposes of characterization of the network structure for medical applications, an ideal network of chains is usually assumed. An ideal network, that is usually assumed a Gaussian network, is with a collection of Gaussian chains between multifunctional junction points (crosslinks). This Gaussian model has two significant assumptions [39.42].

- Crosslinked polymer chains are represented by a Gaussian distribution. This implies that the end to end distance is much smaller than the contour length of the chain.
- Crosslinks, on an average are tetra functional.

1.7.1.1 Real Networks and Network Defects: Real polymer networks always deviate from the ideal Gaussian model.

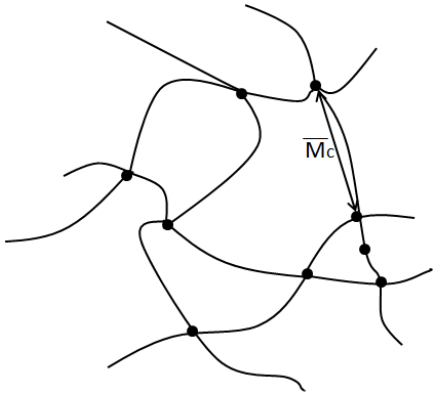

Figure 1: Ideal Gaussian network Mc is the molecular weight betweeen crosslinks [40].

Imperfections can arise for a number of reasons. There might be deviations from the original conditions of crosslinking, crosslinking of already crosslinked networks and end-linking. Imperfections which occur are generally of the following form [39.46]:

- Pre-Existing Order: These types of imperfections include crystallites showing three dimensional structure, non-randomly oriented segment sequences, artificially oriented chains, and micellar and globular structures. These are probably caused due to the association of dissimilar parts of the chain.
- Network Defects: These include closed loops, unreacted functionalities, and chain entanglements
- Inhomogeneities
- Phase Separation Structures: Phase separation occurs when the critical value of crosslinking density is exceeded, because the amount of solvent in the gel has exceeded maximum swelling capacity.

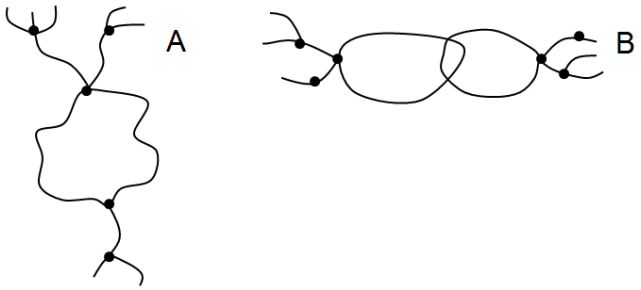

Figure 2: Network Defects (A) Entanglements (B) Loops [40].

1.7.2 Swelling Parameters and Their Significance:

As mentioned earlier, for biomedical purposes, the hydrogel network is considered to be ideal. In order to study the network structure of the hydrogels, it is essential that certain parameters of the gel network are determined. The most important parameters used to characterize network structure are the polymer volume fraction in the swollen state ($v2$,), molecular weight of the polymer chain between two neighboring cross links (M_c), and the corresponding mesh size (ξ). Due to the random nature of the polymerization process, only average values of M_c can be calculated. The polymer volume fraction in the swollen state is a measure of the amount of fluid absorbed and retained by the gel. M_c is a measure of the degree of crosslinking of the polymer, regardless of the nature (physical or chemical) crosslinking. The mesh size, or the correlation distance between two adjacent crosslinks, provides a measure of the space available between the macromolecular chains available for diffusion and movement of particles. This is also an average value. These three parameters can be determined using the equilibrium swelling theory. The three parameters are critical in describing the nanostructure of the crosslinked hydrogels.

- Polymer Volume Fraction: The polymer volume fraction is described as the ratio of the polymer volume (V_p) to the swollen gel volume (V_g). It is also a reciprocal of the volumetric swollen ratio (Q), which can be related to the densities of the solvent (ρ_1) and polymer (ρ_2) and the mass swollen ratio (Q_m) as given by [42.45]:

$$\nu_{2,s} = \frac{V_p}{V_g} = Q^{-1} = \frac{\frac{1}{\rho_2}}{\frac{Qm}{\rho_1}+\frac{1}{\rho_2}} \qquad (1)$$

- Molecular Weight Between Crosslinks: The average molecular weight between crosslinks $\overline{M_c}$, in gels crosslinked during polymerization is given by a modified version of the Flory-Rehner expression [42.48]:

$$\frac{1}{\overline{M_c}} = \frac{1}{\overline{M_n}} - \frac{\left(\frac{\nu}{V_1}\right)[\ln(1-\nu_{2,s})+\nu_{2,s}+\chi_1\nu_{2,s}^2]}{\nu_{2,s}^{1/3}\frac{\nu_{2,s}}{2}} \qquad (2)$$

Here $\overline{M_n}$ is the average molecular weight of the linear polymer chains, ν is the specific volume of polymer, V_1 is the molar volume of water, and χ_1 is the polymer-water interaction parameter.

- Mesh Size: Mesh size can be described using the following equation [42.48]:

$$\zeta = \nu_{2,s}^{\frac{1}{3}}(\overline{r_0^2})^{\frac{1}{2}} = Q^{1/3}(\overline{r_0^2})^{1/2} \qquad (3)$$

$(\overline{r_0^2})^{\frac{1}{2}}$ is the root mean squared end to end distance of network chains between two adjacent crosslinks in the unperturbed state.

Once the nanostructure of the gel is known, a clear idea is obtained about its suitability for use in drug delivery. The amount of liquid retained, the distance between polymer chains, and flexibility of those chains together determine the mobility of the encapsulated molecule and their rates of diffusion within the matrix.

1.8 Swelling Theories

As mentioned earlier, there are different theoretical models used to determine the crosslinking density of a hydrogel. The two most commonly used theories to this end are the equilibrium swelling theory and the rubber elasticity theory [42.48].

1.8.1 Equilibrium Swelling Theory:

This is the most well known model used to calculate the number average molecular weight between crosslinks. It is also known as the Gaussian model (Flory-Rehner). The model is based on two assumptions:

- The crosslinked polymer chains can be represented by a Gaussian distribution.
- The crosslinks on the average are tetrafunctional

As the matrix is swollen by the liquid, the chains between the cross-links become elongated so that a force opposite to the elastic retractive force of the chain develops [42.47]. On further swelling of the polymer matrix, the force increases whereas the thermodynamic force of dilution decreases. This theory states that the thermodynamic force of mixing and the retractive force of the polymer chain come to equilibrium.

$$\Delta G_{total} = \Delta G_{elastic} + \Delta G_{mixing} \qquad (4)$$

Where, $\Delta G_{elastic}$ is the contribution due to the elastic forces developed inside the gel, and ΔG_{mixing} is the result of spontaneous mixing of fluid molecules in the polymer chains, and is a measure of how compatible the polymer is with the molecules of the surrounding fluid.

$$\Delta G_{mixing} = kT[n_1 ln v_1 + n_2 ln v_2 + \chi n_1 v_1] \qquad (5)$$

Where,

n_1 : moles of swelling agent

n_2: moles of polymer

ν_1: volume fraction of swelling agent

ν_2: volume fraction of polymer

K: Boltzmann constant

χ: Flory polymer-solvent interaction parameter.

For a cross-linked system without uncrosslinked polymer chains (n_2 = 0)

$$\Delta G_{mix} = kT[n_1 ln\nu_1 + \chi n_1 \nu_1] \quad (6)$$

The deformation process must occur without appreciable change in the internal energy, thus the internal energy and, therefore, the elastic free energy is defined by:

$$\Delta G_{el} = -T\Delta S_{el} \quad (7)$$

Where, ΔS_{el} is the change in entropy from deformation process. For isotropic swelling, elastic free energy is:

$$\Delta G_{el} = \left(\frac{kT\nu_e}{2}\right)(3\alpha_s^2 - 3 - ln\alpha_s^3) \quad (8)$$

ν_e: effective number of chains in the network

α_s: Expansion factor expressing the linear deformation of a network structure due to isotropic swelling.

The chemical potential of a solvent in a swollen gel is:

$$\mu_1 - \mu_{10} = N(\frac{\partial \Delta G_{mix}}{\partial n_1})_{T,P} + N(\frac{\partial \Delta G_{el}}{\partial \alpha_s})_{T,P}(\frac{\partial \alpha_s}{\partial n_1})_{T,P} \quad (9)$$

And N is Avogadro‟s number.

Also,

$$\alpha_s^3 = \frac{1}{\nu_2} = \frac{(V_0 + \frac{n_1 V_1}{N})}{V_0} \quad (10)$$

V_0: molecular weight of the network before swelling

V_1: molar volume of the swelling agent

Peppas and Merrill modified the above original Flory-Rehner model for hydrogels prepared in the presence of water. The presence of water modifies the change of chemical potential due to elastic forces. There must now be a term which accounts for the volume fraction density of the chains during crosslinking. The equation below predicts the molecular weight between crosslinks in a neutral hydrogel prepared in the presence of penetrant [42.48]:

$$\frac{1}{M_c} = \frac{1}{M_n} - \frac{\left(\frac{\nu}{V_1}\right)[\ln(1-\nu_{2,s})+\nu_{2,s}+\chi_1\nu_{2,s}^2]}{\nu_{2,r}\left[\left(\frac{\nu_{2,s}}{\nu_{2,r}}\right)^{\frac{1}{3}}-\left(\frac{\nu_{2,s}}{2\nu_{2,r}}\right)\right]} \qquad (11)$$

Where $\nu_{2,r}$ is polymer volume fraction in the relaxed state (after crosslinking, before swelling).

1.8.2 Rubber Elasticity Theory:

The other theory used to determine crosslinked structure of a gel is the rubber elasticity theory. Hydrogels resemble natural rubbers in their property to elastically respond to applied stress. Thus when a crosslinked network is stretched, it reaches an equilibrium strain while the stress remains constant [42.51]. A hydrogel subjected to small deformation, less than 20% will fully recover to its original dimension rapidly. The rubber elasticity theory is used to explain this behavior, thermodynamically. This theory was first developed by Treolar and Flory for vulcanized rubbers and modified to polymers. Later expressions were developed which apply to hydrogels prepared in presence of solvent [42.46].

According to the modified theory for hydrogels prepared in presence of solvent, we have [42.48]:

$$\tau = \frac{\rho RT}{\overline{M_c}} - \left(1 - \frac{2\overline{M_c}}{\overline{M_n}}\right)(\alpha - \frac{1}{\alpha^2})(\frac{\nu_{2,s}}{\nu_{2,r}})^{\frac{1}{3}} \qquad (12)$$

Here τ is the stress applied to the polymer sample, ρ is the density of the polymer, R is the universal gas constant, T is the absolute experimental temperature, and $\overline{M_c}$ the average molecular weight between crosslinks.

To be able to analyze the structure of the hydrogel using this theory, experiments need to be performed using a tensile system. This theory can be used to analyze chemically, physically crosslinked as well as hydrogels exhibiting temporary crosslinks due to hydrogen bonding.

1.8.3 Calculation of Mesh Size:

The mesh size defines the space between macromolecular chains in a crosslinked network, and is characterized by the correlation length, ξ between two adjacent crosslinks. The calculations for the mesh size can be conducted as follows using the following equations [42.48]:

$$\zeta = \alpha(\bar{r}_0^{1/2})^2 \qquad (13)$$

Here α is the elongation ratio of the polymer chains in any direction, and $(\bar{r}_0^{1/2})^2$ is the root mean square, unperturbed end to end distance of the polymer chains between two neighboring crosslinks.

For isotropically swollen hydrogels, α is related to the polymer volume fraction $\nu_{2,s}$ as follows [42.48]:

$$\alpha = (\nu_{2,s})^{-1/3} \qquad (14)$$

$(\bar{r}_0^{1/2})^2$ can be calculated using the following equation [42.44]:

$$(\bar{r}_0^{\frac{1}{2}})^2 = l(C_n N)^{1/2} \quad (15)$$

Where C_n the Flory characteristic ratio is l is the length of the bond along the polymer backbone, and N is the number of links that is calculated using [42.45]:

$$N = \frac{2\bar{M}_c}{M_r} \quad (16)$$

Mr is the molecular weight of the repeating units from which the polymer chain is composed. When one combines the above equations Eq (14), (15), (16) and rearranges them, we obtain the equation for calculation of the mesh size in a swollen hydrogel [42.48]:

$$\zeta = (\nu_{2,s})^{-1/3}(\bar{r}_0^{1/2})^2 \quad (17)$$

Thus calculation of the mesh size and other swelling parameters allow for proper design and characterization of diffusion of model drugs and proteins into the complex structure of gels.

1.9 Mechanical Properties

The mechanical integrity over the life span of a system is an important consideration when designing a successful biomedical device. Changing the molecular weight between crosslinks and copolymerization has both been utilized to achieve desired mechanical properties. Some applications may necessitate mechanical properties that change over time. This is the case with many of the degradable scaffold systems for tissue engineering where the device must have significant strength initially but degrade as cellular material

is incorporated [46.58]:. One of the main considerations for drug delivery systems is that the device protects the incorporated drug until it is released. Compressive modulus has been shown to be as low as 1 kPa for a variety of drug delivery devices

It has been well documented that the mechanical properties of hydrogels are highly dependent on network chemistry and molecular weight between crosslinks. While mechanical strength measurements can be used to confirm that a device is suitable for a specific application they can also be used to evaluate the effects of changes in the network chemistry and to monitor the degradation behavior of gels [52.58]:. Two factors are expected to influence the mechanical properties in the PEG and triblock hydrogels. The first factor is the change in molecular weight between crosslinks that comes with different PEG molecular weights, both in the PEG gels and the triblock gels. The second factor is the incorporation of another segment (i.e., biodegradable segment) into the network, which is a stiffer, more hydrophobic group. It has been shown that as PEG molecular weight increased the gels were able to swell more and thus had a lower compressive modulus. Specifically, as the PEG molecular weight increased, the compressive modulus decreased in non-degradable gels. The same reduction in compressive modulus was present for degradable gels [54.60]:

1.10 Bioegradable Hydrogels

Since the appearance of synthetic polymers 60 years ago, medical professionals rapidly realized that these materials could be interesting for therapeutic applications. A great number of polymers have been evaluated as potential biomaterials due to the great

variety of their compositions, structures, and properties that cover a wide range of applications [42.55].

Polymeric biomaterials can be divided in two groups. The first group is those for permanent aids such as protheses. In contrast, the second group is used for temporary aids that are needed for only a limited period of time and are based on the capacity of living systems to self-repair. Biodegradable implants are advantageous over other implants because they do not have to be surgically removed once their presence is no longer needed. Biodegradable implants should effectively degrade and eventually be resorbed or excreted by the body. Degradable implants can circumvent some of the problems associated with the long-term safety of permanently implanted devices as well. Since implantable drug delivery devices are by nature temporary devices, the development of implantable drug delivery systems is probably the most widely investigated application of degradable polymer systems. Degradable polymers are of great interest for temporary therapeutic applications such as wound closure, tissue repair and regeneration, and drug delivery. Degradable hydrogels in particular are desirable for a variety of applications; for example, tissue engineering scaffolds that can be degraded and remodeled as the cells migrate and synthesize new extracellular matrix are thought to allow more successful long-term tissue regeneration. In cell-based therapies and protein delivery applications, hydrogel degradation can be used to control the release rate of the delivered component and also permit clearance of the device from the body when it is no longer needed [58.62].

1.10.1 Biodegradable polymers

1.10.1.1 Poly (Lactic Acid) and Poly (Glycolic Acid)

Most degradable polymers contain in their backbone labile linkages such as esters, orthoesters, anhydrides, carbonates, amides, urethanes, ureas, etc. However, aliphatic polyesters containing flexible ester bonds, and those derived from lactic acid (LA) and glycolic acid (GA) in particular appear to be the most promising because of their excellent biocompatibility and variable degradability. High molecular weight poly(LA) (PLA) , poly(GA) (PGA) and their copolymers are obtained by the ring-opening polymerization of cyclic diesters, which are lactides and glycolide. In the case of LA-containing polymer chains, the chirality of the LA units provides a worthwhile means to adjust degradation rates, as well as physical and mechanical properties. This nomenclature presentsthe advantage of clearly reflecting the chemical and configurational compositions of the polymers, the average polymer chain composition being generally close to that of the feed.

The *in vivo* and in vitro degradations of PLAGA polymers have been extensively investigated during the past two decades. It was established that degradation is catalyzed by carboxyl end groups formed by chain cleavage and that amorphous regions are preferentially degraded. Nevertheless, a lot of discrepancies or controversial data existed in the literature, especially concerning the degradation rates, degradation location (at the surface or in the bulk), and the involvement of enzymes *in vivo.*

1.10.1.2 Polydioxanone and Polycaprolactone

Polydioxanone (PDS) is a bioabsorbable polymer that was first developed specifically for wound closure sutures. The compatibility, degradation rate, and mechanical properties (including shape memory) of PDS are of interest when considering the design of tissue engineering scaffolds. As a suture material, it exhibits high flexibility,

irrespective of the diameter, and higher strength retention, slower absorption rates, and lower inflammatory response rates when compared to PLGA and PGA. PDS has been used in orthopedics, plastic surgery, drug delivery, cardiovascular applications, and bone repair applications. These other applications have had mixed results which has slowed the expansion of PDS applications [60.65].

Polycaprolactone (PCL) receives less attention in the field of orthopedics due to the lack of functional groups which can be used for surface tailoring. Poly(ε-caprolactone) is known to be biocompatible, slowly hydrolytically and enzymatically degradable and has been used in long term medical applications. Its physical properties and commercial availability make it very attractive as a specific plastic of medicine and agricultural areas. The main limitation of PCL is its low melting temperature.

1.10.2 Degradation Mechanism

The degradation mechanism of PLAGA polymers has been investigated by many researchers. In general, degradation is considered to be a hydrolytic process. The cleavage of an ester bond yields a carboxyl end group and a hydroxyl one. Thus, the formed carboxyl end groups are capable of catalyzing hydrolysis of other ester bonds, a phenomenon called autocatalysis. A few years ago, the discovery of faster degradation inside large-sized PLA_{50} specimens greatly changed the understanding of the hydrolytic degradation of PLAGA polymers. This phenomenon was first discovered by visually examining the degraded specimens. For example, after 5 weeks of degradation in the phosphate buffer, the cross section of a PLA50 specimen became heterogeneous, the interior being composed of viscous oligomers. After 12 weeks, the interior totally

disappeared, and only the shell remained. *In vivo* degradation led to similar findings. After 2 weeks the PLA_{50} specimen also showed a surface–interior differentiation. After 2 months the interior disappeared [62.65].

The heterogeneous degradation was assigned to reaction–diffusion processes as summarized in the following. Initially, the polymer matrix is homogeneous in the sense that the average MW is the same throughout the matrix. Once placed in an aqueous medium, water penetrates into the specimen, leading to hydrolytic cleavage of ester bonds. Each ester bond cleavage forms a new carboxyl end group that, according to autocatalysis, accelerates the hydrolytic reaction of the remaining ester bonds. At the very beginning, degradation occurs in the bulk and is macroscopically homogeneous. However, the situation becomes totally different when soluble oligomeric compounds are generated in the matrix. The soluble oligomers that are close to the surface can escape from the matrix before total degradation, while those located inside the matrix can hardly diffuse out of the matrix. This difference results in a higher acidity inside than at the surface. When the aqueous medium is buffered at neutral, as is the case in a pH 7.4 phosphate buffer or *in vivo*, the neutralization of carboxyl groups present at the surface also contributes to the decrease of the surface acidity. Therefore, autocatalysis is larger in the bulk than at the surface, thus leading to a surface–interior differentiation. As the degradation proceeds, more and more carboxyl end groups are formed inside to accelerate the internal degradation and enhance the surface–interior differentiation. Bimodal MW distributions are observable that are due to the presence of two populations of macromolecules degrading at different rates. Finally, hollow structures

are formed when the internal material, which is totally transformed to soluble oligmers, dissolves in the aqueous medium [59.65].

1.10.3 Degradation Charactersitics

Each degradable polymer family presents particular characteristics during degradation, in spite of the common degradation mechanism. In fact, degradation results from a complex process that depends on many factors such as matrix morphology and chain orientation, chemical composition and configurational structure, distribution of chemically reactive compounds within the matrix, MW, the presence of residual monomers and oligomers, size and shape, γ irradiation, and degradation media. The influence of these factors on polymer degradation is discussed in the following.

1.10.3.1 Polymer Morphology: The morphology of a polymeric material (i.e., amorphousness or semicrystallinity) plays a critical role in the degradation process. It is now known that degradation of semicrystalline polyesters in aqueous media occurs in two stages. The first stage consists of water diffusion into the amorphous regions with random hydrolytic scission of ester bonds. The second stage starts when most of the amorphous regions are degraded. The hydrolytic attack then progresses from the edge toward the center of the crystalline domains.

Chain orientation in crystalline and amorphous regions could also play an important role in the degradation of polymers. In the case of melt-spun fibers, for example, alternative crystalline and amorphous regions arrange in the direction of the fiber axis. Two types of tie-chain segments (i.e., interfibrillar and intrafibrillar) are present in the amorphous regions of the microfibrillar structure. Their major function is

to tie crystalline regions together and to transmit tensile loads. As proposed by Chu, the scission of these tie-chain segments leads to rapid loss of tensile properties and higher chain mobility. Chain orientation along the fiber axis renders the fiber material less susceptible to water penetration and more resistant to hydrolytic attack. Unfortunately, water absorption or weight loss data are not available. Ginde and Gupta examined the degradation of PGA fibers and pellets of comparable crystallinities. Degradation of pellets was much faster than that of fibers. The difference was assigned to the presence of long-range order in fibers. Nevertheless, degradation of large-sized pellets could also have been enhanced by autocatalysis, which was not the case of slim fibers [53.59].

It is also worthwhile to note the presence of imperfections and defected crystalline regions. When the spherulitic crystallization develops within a matrix containing impurities, monomers, or oligomers, these noncrystallizable species are often concentrated at the interspherulitic boundaries. Chu suggested that because of the existence of these defects, a few portions of the crystalline regions could also be destroyed simultaneously, but more slowly, during the degradation of the amorphous regions. Consequently, a strict demarcation of the second stage of degradation from the first one is difficult to assess.

1.10.3.2 Influence of Initial Crystallinity on Degradation Rate: PLA is an intrinsically semicrystalline polymer. In order to examine the influence of the initial crystallinity on the degradation rate, investigations were carried out comparatively on an amorphous PLA_A obtained by quenching and a semicrystalline PLA_C obtained by annealing. The crystallinity of PLA_C was 72%, which was deduced from X-ray diffraction. Weight loss data showed that, during the first 18 weeks, PLA_A did not lose

any material. After 30 weeks, nearly 4% of the weight was lost, thus showing the release of soluble oligomers produced by degradation. Beyond that time the weight loss continued to increase and reached almost 50% at 110 weeks. In the PLA_C a small weight loss was detected after 7 weeks, which was earlier than in the PLA_A. Nevertheless, the increase of weight loss was slower. At the end of 110 weeks, only 26% of the material was lost. Therefore, the crystallinity reduced the overall degradation rate of PLA in terms of weight loss [42.50].

1.10.4 Degradation and Swelling behavior

It has already been shown that the addition of lactide blocks to the ends of PEG chains changed the properties of the polymer. Lactide blocks were also expected to have an effect of the properties of the hydrogels; primarily the degradation of the gels over time. The swelling for degradable gels is more complex than for non-degradable gels. In non-degradable gels the water diffuses into the network, pushing the chains apart, causing swelling. When the water diffusing into the gel is balanced by the stretching of the chains, equilibrium is reached and no further swelling occurs. In degradable gels, the water diffuses into the system pushing the chains apart but at the same time the water begins to degrade parts of the gel. One scission point along the backbone will result in dangling chains that do not provide the same resistance to swelling as connected sections. Two scission points will result in that segment of the polymer chain entering into solution in the aqueous surroundings. This in effect increases the molecular weight between crosslinks, which allows the gel to uptake more water. Also, the addition of more rigid, hydrophobic blocks is expected to affect the hydrogels ability to swell, which will in turn affects the degradation of the gels. Each of the parameters that were

evaluated for the PEG hydrogels have also been evaluated for degradable triblock gels to determine the effect of lactide blocks on swelling and degradation [32.40].

1.11 PEG Based Hydrogels

One of the most studied and widely applied hydrogels is poly(ethylene glycol) (PEG). PEG has been explored as cell scaffolds as well as drug delivery devices. PEG has many properties that make it an excellent candidate as a biomaterial. PEG is soluble in water and many organic solvents including toluene, methylene chloride, ethanol, and acetone. PEG is nontoxic, has a rapid clearance from the body, and has been approved for several medical applications. One of the most important properties is that PEG resists recognition from the immune system. It also resists protein and cell adsorption. Covalent bonding of PEG to other molecules may enhance the properties of other molecules rendering them nonimmunogenic, water soluble, and protein rejecting. These molecules not only exhibit many of the properties of PEG, but they retain their biological activity. Because of the high mobility of PEG, molecules that are tethered to it exhibit activity similar to that of a freely soluble molecule. The proteins that are tethered to PEG are not denatured, and because their size is increased, their rate of clearance through the body is often increased. However, PEG by itself is nonreactive and to create insoluble networks, it requires end-functionalization with cross-linking groups. A number of chemistries have been developed for the functionalization of PEG including the addition of acrylate, thiol, amine, maleimide, or vinyl sulfone (VS) reactive groups. As crosslinked networks, these materials are nondegradable under physiological conditions [12.20].

To facilitate degradation in PEG-based hydrogels, a number of strategies have been developed that utilize degradable blockcopolymer components (e.g., poly (lactic acid) (PLA)). One family of PEG-based degradable hydrogels is based on the copolymer PLA-b-PEG-b-PLA dimethacrylate. Despite its many successful applications, this type of hydrogel structure can be associated with drawbacks such as protein denaturation due to the PLA hydrophobicity and inflammation caused by acidic degradation byproducts of PLA such as lactic acid and poly(acrylic acid). Multiarm PEG-amine cross-linked with an ester-containing amine-reactive PEG derivative has also been utilized as a hydrolytically degradable PEG scaffold for protein delivery This polymer is fully hydrophilic, but its application is restricted because the amine reaction allows covalent binding of encapsulated proteins to the polymer network during cross-linking. This issue had been circumvented by the use of PEGmultiacrylates and PEG-dithiols to form a fully hydrophilic hydrogels with selective cross-linking chemistry [31.39].

1.12 Star Polymer Based Hydrogels

Star polymers are three-dimensional hyperbranched structures in which linear arms of the same or different molecular weights emanate from a central core. The existence of numerous functional groups in a small volume makes these polymers important for use in biological and pharmaceutical applications. Biologically active molecules can be immobilized on the surface of the polymer gel or incorporated into the network [42.59].

2. Aim of This Research

The objective of this work was to develop a way to allow the 4-arm PEG gels to be degradable via hydrolysis, a process that does not require the presence of specific biological compounds, such as proteases. One method of accomplishing this goal was copolymerization of PEG with degradable hydroxyl acid (HA) monomers. However, the hydrophobicity of degradable segments decreases the water solubility of the macromonomer dramatically. For this reason, our aim was to add very short segments of hydrolysable monomers to PEG molecules to preserve the water solubility of PEG while allowing for the degradation of the whole molecule. Moreover, the addition of the hydrophobic monomers results in the formation some micellar structure in the precursor solution which affects the properties of the final gel.

According to prior works, we hypothesized that the hydrogel properties would depend on several factors including type and molecular weight of the degradable segment, and also the macromonomer concentration. In order to test this hypothesis, we successfully synthesized various macromonomers from 4-arm PEG bearing short sequences of poly (ε-caprolactone) (C), poly (pdioxaone) (D), poly (L-lactide) (L) and poly (glycolide) (G) at each end using ring opening polymerization. Also, we investigated the impact of these factors on the hydrolytically degradation, mechanical

strength, water content and sol fraction of hydrogels fabricated by 4-arm poly (ethylene oxide-co-X) acrylate (SPEXA) macromonomers which X=C, D, L and G. In addition, the properties of SPELA hydrogels was compared to the linear poly (ethylene oxide-co-lactide) acrylate (LPELA) to investigate the effect of molecular structure on hydrogels properties.

3. Experimental Design

3.1 Macromonomers Synthesis

Ring opening polymerization (ROP) of dioxanone (D), caprolactone (C), glycolide (G) and lactide (L) was used for the synthesis of SPED, SPEC, SPEG, SPEL and LPEL, respectively, in the presence of star poly (ethylene glycol) or linear poly (ethylene glycol) as the reaction initiator and TOC as the polymerization catalyst, as described previously. For the synthesis of SPEX (X=C, L and G) or LPEL, dry PEG and the monomer were added to a three-neck flask with an overhead stirrer and immersed in an oil bath. In order to control the length of the degradable segments of the macromer, various molar ratios of the monomers to PEG (15, 10, 7.5 and 5) were used. In the case of X= C or L, the reaction flask was then heated up to 120°C under nitrogen stream to melt the mixture and see a colorless viscous liquid. After maintaining the temperature for 1 h to remove any potential moisture, the catalyst was added to the mixture and the temperature was increased to 140°C. The reaction was run at 140°C over 8 h. When X=G, the reaction was carried out at 160°C for 10 h. For the synthesis of SPED, the mixture of initiator and catalyst was heated up to 130°C and kept at this temperature for an hour to remove the moisture and the mixture was then cooled down to 85°C (corresponding to a high conversion in the

ROP of dioxanone) and the monomer was then added to the system. This reaction was then run at this temperature for 48 h. After completion of the reactions, the products were precipitated in ice cold hexane to remove any unreacted monomer, initiator and catalyst. In the next step, the end-groups of the macromer were acrylated to produce SPEXA. The product of the previous reaction was dissolved in DCM and dried with azeotropic distillation from toluene, in order to remove any residual moisture. Then, the macromer was dissolved in DCM and the reaction flask was immersed in an ice bath to control the reaction temperature. The equimolar amounts of acryloyl chloride and TEA (equal to the total number of moles of macromer chain ends) were added drop-wise to the macromer solution under nitrogen stream. The reaction was stopped after 12 h. Then, the solvent was removed using rotary evaporation and the residue was dissolved in ethyl acetate to precipitate the byproduct of triethylamine hydrochloride salt. After removing the ethyl acetate using vacuum distillation, the macromer was re-dissolved in DCM and precipitated in ice cold ethyl ether twice. Then, the product was dissolved in dimethylsulfoxide (DMSO) and dialyzed against water to remove any remaining impurities. Finally, the SPEXA product was dried in vacuum to remove residual solvent and stored at –40°C.

3.2 Macromonomer Gelation and Rheological Measurements

Free-radical UV polymerization was used to crosslink the aqueous solution of the macromonomers in the presence of 4-(2-hydroxyethoxy)phenyl-(2-hydroxy-2-propyl) ketone (Irgacure 2959; CIBA, Tarrytown, NY) as a water soluble photoinitiator used for water-based UV formulations. The photoinitiator was dissolved in distilled deionized (DI) water by alternating between agitation and

heating to 50°C to prepare a homogeneous and clear solution. Various concentrations of precursor solution were prepared by adding the photoinitiator solution to the macromonomer. For example, in order to prepare 300 µl precursor solution with a concentration of 20 wt%, 60 mg polymer was dissolved in 240 µl photoinitiator solution. The concentration of photoinitiator in all of the precursor solutions was 0.75 wt% because of the low cells toxicity, optimum mechanical property, and gelation time.

In order to measure the mechanical strength of the hydrogels, a rheometer (TA Instruments, New Castle, DE) with a 20 mm plate acrylic geometry to monitor the crosslinking reaction. The precursor solutions were then loaded on the Peltier plate of the rheometer as shown in the Figure 3. The gap distance between the geometry and the peltier plate was kept in 500 µm for all the experiments. A sinusoidal shear strain profile was exerted on the samples via the upper geometry at a constant frequency of 1 Hz while the samples were irradiated with a BLAK-RAY 100-W mercury long wavelength (365 nm) UV lamp (Model B100-AP; UVP, Upland, CA) 4-6. The UV exposure time for all samples was 1000 s. The storage and loss moduli (G' and G") of the samples were recorded with irradiation time.

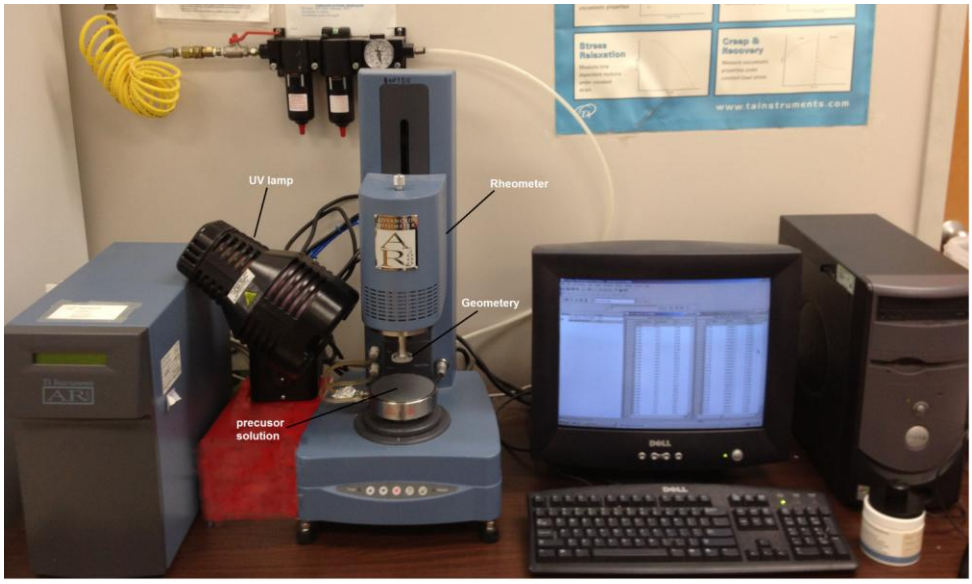

Figure 3: Rheometer used for mechanical test

One of the more common definitions of hydrogel is that a gel consists of two components, a solid and a liquid, where the solid is the minority component and the liquid the majority component. The solid phase extends through the entire volume of the gel. In a recent review, a gel is defined as a system of molecules, particles, chains, etc. which are partially connected to each other in a fluid medium. A more detailed definition can be derived from the rheological properties of the gel systems. Almdal and Kramer defined that the storage modulus G' should be independent of the frequency at least on the order of seconds and the loss modulus G" should be considerably lower than the storage modulus. However, some systems do not follow all of these criteria, e.g. the storage modulus is only slightly higher than the loss modulus even though the gel appears to be free-standing. These systems have been characterized as “weak” gels. The most commonly used definition of hard or weak gels goes back to the work of Hvidt et.al., who categorized gels with a storage modulus on the order of 104 Pa as “hard” gels and gels with a storage modulus on the

order of 101 Pa as “weak” gels. The critical point for differentiation between “hard” and “soft” gels was defined as the threshold of 103 Pa. Therefore, the gelation time is defined as point that G' and G" are equal and after that point G' is greater than G" as can be seen in the Figure 4.

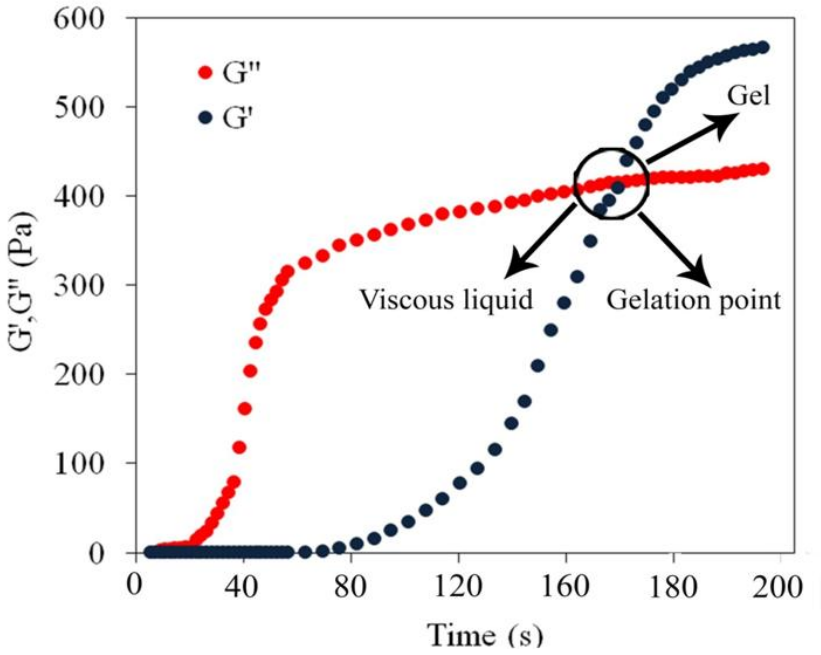

Figure 4: Variation of G’ and G” with time.

In order to measure the compressive modulus (E), first circular hydrogels with a diameter of 20 mm and a thickness of 500 µm were fabricated by irradiating the precursor solution for 1000 s. The samples were then loaded under the geometry to apply a vertical force to reach the breaking point and record the variations of stress against strain at a strain rate of 0.02 s^{-1}. In order to calculate the elastic modulus, the slope of the initial linear part of stress-strain curve was considered as shown in the Figure 5.

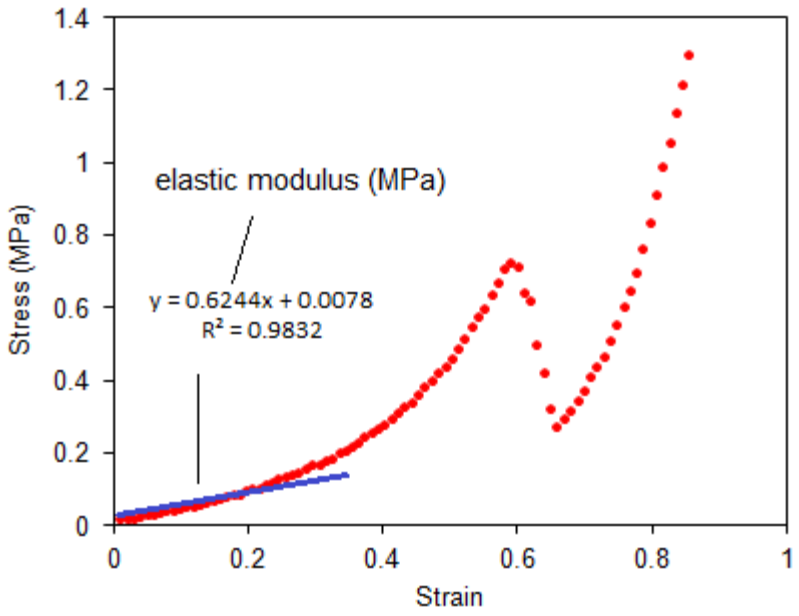

Figure 5: Stress vs strain graph for calculation of elastic modulus

3.3 Measurement of Swelling Ratio and Sol Fraction

After crosslinking, samples with a diameter of 20 mm and a thickness of 500 µm were removed from the Peltier plate of the rheometer to measure their swelling ratio and sol fraction. The samples were dried in ambient conditions for 12 h followed by drying in vacuum for 1 h at 40°C. The dry weights (w_i) were then recorded. Next, the dry samples were swollen in DI water for 24 h at 37°C changing the swelling media every 6 hours. After swelling, the surface water was removed and the swollen weights (w_s) were measured. Then, the swollen samples were dried as described above and the dry weights (w_d) were recorded. The following equations were used to calculate the weight swelling ratio (Q) and sol fraction (S):

$$Q = \frac{w_s - w_d}{w_d} \times 100 \qquad (18)$$

$$S = \frac{w_i - w_d}{w_i} \times 100 \qquad (19)$$

3.4 Measurement of degradation

The macromonomer precursor solutions were degassed, transferred to a PTFE mold (5 cm × 3 cm × 500 μm), covered with a transparent glass plate, fastened with clips, and UV crosslinked for 1000 s. Disc shape samples were cut from the gel using an 8 mm cork borer and dried under vacuum to record the initial dry weight. The mass loss was measured in primary culture media (5 ml per sample) without fetal bovine serum at 37ºC and under mild agitation. The primary media was prepared by dissolving 13.4 g of Dulbecco's Modified Eagle Medium (DMEM; 4.5 g/l glucose with Lglutamine and without sodium pyruvate; Mediatech, Herndon, VA) in 900 ml of DI water containing 3.7 g sodium bicarbonate and 10 ml antibiotic and antimycotic agents (1% v/v). At each time point samples were removed from the media, washed with DI water three times to remove the excess salts and dried under vacuum. The time point steps for SPEXA (X=C, D and L) and LPELA were every three days while they were every six hours in the case of X=G because of the fast degradation rate. The dried sample weights were then measured and compared with the initial dry weights to determine the fractional mass remaining.

3.5 Cell Study

3.5.1 Bone Marrow Stromal Cell (MSC) Encapsulation in the Hydrogels

MSCs were isolated from the bone marrow of young adult male Wistar rats. Cell isolations were performed under a protocol approved by the Institutional Animal Care and Use Committee of the University of South Carolina. The bone marrow cell suspensions were centrifuged at 200g for 5 min, and cell pellets were resuspended in 12

mL of basal medium (DMEM supplemented with 10% FBS, 100 units/mL penicillin (PEN), 100 μg/mL streptomycin (SP), 50 μg/μL gentamicin sulfate (GS), and 250 ng/mL fungizone (FZ)) and aliquoted into T-75 flasks. The flasks were subsequently maintained in a humidified 5% CO2 incubator at 37 °C. Cultures were replaced with fresh medium at 3 and 7 days to remove hematopoietic and other unattached cells. After 10 days, cells were detached from the flasks with 0.05% trypsin-0.53 mM EDTA and used for in vitro experiments.

SPEXA-nX0 (a) SPECA-nC7.2 (b), SPEDA-nD6.8 (c) and SPELA-nL6 were selected for encapsulation and osteogenic differentiation of MSCs as the optimum molar ratio of degradable segments to the PEG (XEGF). SPEXA-nX0 (a) SPECA-nC7.2 (b), SPEDA-nD6.8 (c) and SPELA-nL6 macromonomers was dissolved in PBS by correlating the concentration with the constant compressive modulus value (50 kPa) and sterilized by filtration with a 0.2 μm filter. Acrylamide-terminated GRGD peptide (Ac-GRGD) was synthesized on Rink Amide NovaGel resin in the solid phase, purified by HPLC, and characterized by electrospray ionization (ESI) mass spectrometry, as previously described. To the macromonomer solution, 2 wt % Ac-GRGD (based on SPEG, SPELA, SPECA, and SPEDA) was added to improve cell viability and cell-matrix interaction after MSC encapsulation. $1*10^6$ MSCs, suspended in 100 μL of PBS, were added to the SPEXA macromonomer precursor solutions and mixed gently with a presterilized glass rod. The final density of MSCs in the gel was $5*10^6$ cells/mL. The mixture was injected between two sterile microscope glass slides and cross-linked by UV irradiation. The UV exposure time for all samples was 200 s, the minimum time for the gels to reach their plateau modulus. After cross-linking, disk shape samples were incubated in 2 mL of PBS

for 1 h with the PBS two additional times. Next, the medium was replaced with the osteogenic culture medium, and the encapsulated MSCs were incubated for 28 days. Experimental groups included SPEXA-nX0 gels with MSCs incubated in osteogenic media (control), SPELA gels, SPECA gels, and SPEDA gels with MSCs incubated in osteogenic media. For cell viability, disks were stained with cAM/EthD live/dead assay (1μg/mL) to image live and dead cells, respectively. Stained samples were imaged with a Zeiss confocal laser scanning microscope (510-Meta CSLM). At each time point, DNA content (cell number), calcium content, and total collagen content were measured.

3.5.2 Biochemical Analysis for DNA Content, Calcium Concentration and Total Collagen Content

At each time point (7, 14, 28 days), MSC encapsulated SPEXA gels were washed with serum-free DMEM for 8 h to remove serum components, washed with PBS, lysed, and sonicated to rupture the encapsulated cells. Next, the supernatant was used for measurement of DNA content, calcium content, and total collagen content. Analysis of dsDNA was performed using a Synergy HT plate reader (Bio-Tek, Winooski, VT, USA) with emission and excitation wavelengths of 485 and 528 nm, respectively[8]. In order to measure the total mineralized deposit in the gels, Calcium content was measured using a QuantiChrom Calcium Assay kit with a plate reader at 575 nm, as described [8]. Total collagen content was analyzed by SIRCOL collagen assay kit protocol (Biocolor, Newtownabbey, UK) in the sonicated cell lysate of the ruptured samples according to manufacturer's instructions. This method is based on the selective binding property of the [Gly-X-Y] tripeptide end sequence of the collagen to the Sircol dye. In order to measure the total collagen content, 1 mL of Sircol dye was added to the sonicated cell lysate, and

incubated for 30 min and centrifuged at 10,000 rpm for 5 min to separate off the collagen–dye complex formed. After removing the supernatent, 1 mL Sircol alkali reagent mixed with the collagen-dye complex and vortexed. Next, 200 µl of the acquired solution was read at 555 nm. The amount of collagen was calculated based on a standard curve of previously known concentrations of type I collagen measurement.

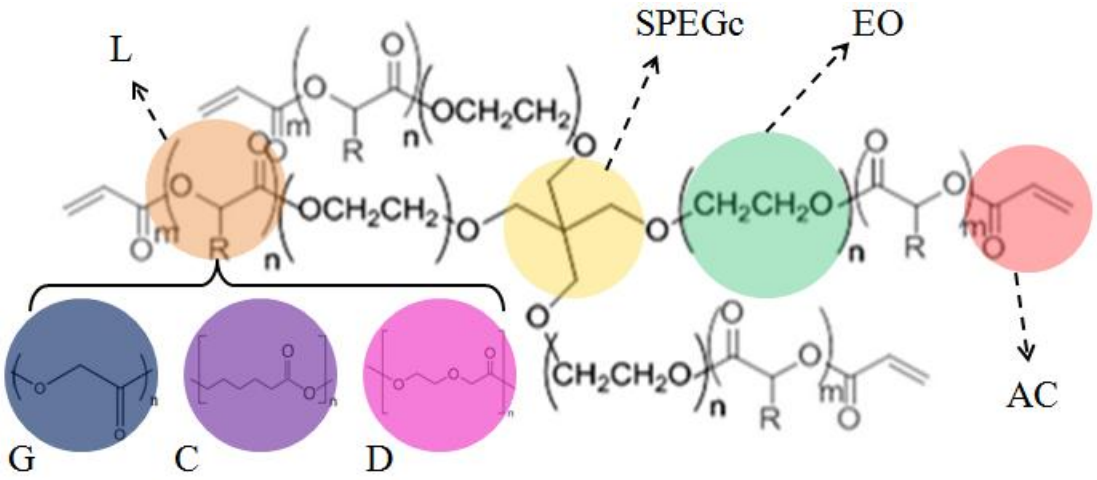

Figure 6: The chemical structure of SPELA, SPEGA, SPECA and SPEDA macromonomers.

4. Results

4.1 Macromonomers Characterization

Spectra of SPEXA-nX (X=C, D, G and L) macromonomers are shown in Figure 7. In Figure 7a, the chemical shifts with peak positions at 3.6 and 4.3 ppm were attributed to the methylene hydrogens of PEG attached to ether and ester groups of lactide respectively. The shifts with peak positions at 1.4, 1.7, 2.3 and 4.1ppm were attributed to the γ, β, α, ε methylene of caprolactone respectively. In Figure 7b, the chemical shifts with peak positions at 3.6 and 4.3 ppm were attributed to the methylene hydrogens of PEG attached to ether and ester groups of dioxanone respectively. The shifts with peak positions at 3.7, 4.2 and 4.4 ppm were attributed to the β, α, γ methylene of dioxanone respectively. In Figure 7c, the chemical shifts with peak positions at 3.6 and 4.3 ppm were attributed to the methylene hydrogens of PEG attached to ether and ester groups of lactide respectively. The shifts with peak positions at 1.6 and 5.2 ppm were attributed to the methyl and methine of lactide respectively. In Figure 7d, the chemical shifts with peak positions at 3.6 and 4.3 ppm were attributed to the methylene hydrogens of PEG attached to ether and ester groups of glycolide respectively. The shifts with peak positions at 4.8-4.9 ppm were attributed to the methylene of glycolide. The shifts with peak positions from 5.85 to 6.55 ppm (see the inset in Figure 7) were attributed to the vinyl hydrogens of the acrylate group at the end of macromonomer arms as follows: Peak

positions in the 5.82-5.87 ppm range were associated with the trans proton of unsubstituted carbon of the Ac; those in the 6.10-6.20 ppm range corresponded to the protons bonded to monosubstituted carbon of the Ac; and those in the 6.40-6.46 ppm range were associated with the proton of unsubstituted carbon of the acrylate group. The ratio monomer to PEG in SPECA, SPEDA, SPELA and SPEGA was determined from the ratio of the shifts centered at 1.4, 1.7, 2.3 and 4.1ppm (caprolactone hydrogens), 3.7, 4.2 and 4.4 ppm (dioxanone hydrogens), 1.6 and 5.2 ppm (lactide hydrogens) and 4.8-4.9 ppm (glycolide hydrogens) to those at 3.6 and 4.3 ppm (PEG hydrogens). The number of acrylate groups per macromonomer was determined from the ratio of the shifts between 5.85 and 6.55 ppm (acrylate hydrogens) to those at 3.6 and 4.2 ppm (PEG hydrogens). The number average of monomers (nX) and acrylate groups per end group of the macromonomers, and $\overline{M_n}$ of the SPEXA macromonomers (X=C, D and G) as a function of molar ratio of monomers and PEG in the feed (XEGF) have been shown in Table 1. The number of monomers per end group of the SPEXA varied from 0.7 to 2.8 for X=C, 0.6 to 2.9 for X=D, 0.8 to 2.9 for X=L and 0.7 to 2.8 in the case of X=G as the XEGF ratio (X= C, D, L and G) was changed from 5 to 15.

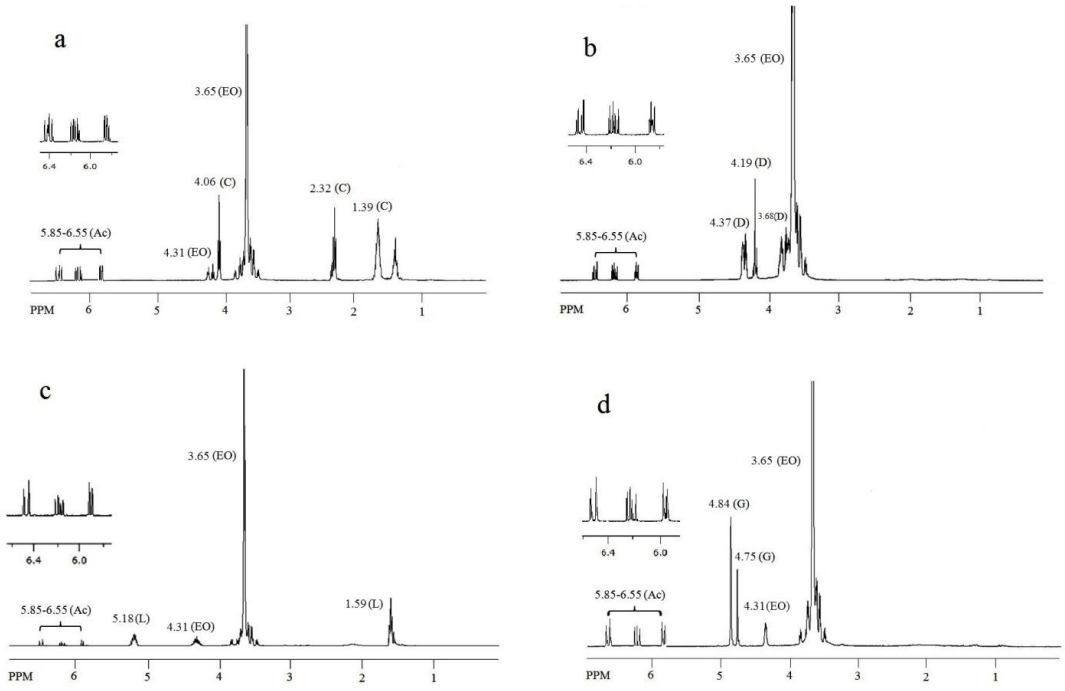

Figure 7: ^{1}H-NMR spectrum of SPECA-nC7.2 (a), SPEDA-nD6.8 (b) and SPELA-nL6.4 (c) SPEGA-ng6.4 (d) macromonomer.

Also, the average number of acrylates per end group of the SPEXA macromonomers were decreased from 0.85 to 0.75, 0.82 to 0.73, 0.86 to 0.74 and 0.86 to 0.78 for X=C, D, L and G, respectively and that of SPEXA-0nX (XEGF=0) is 0.85. In addition, by increasing the XPEG ratio from 5 to 15, of SPEXA was increased from 55 to 64 kDa, 54 to 63 kDa , 5700 to 6900 kDa and 56 to 65 kDa when X= C, D, L and G, respectively.

The number of lactide monomers (nL) and functional acrylate groups per macromonomer, and the $\overline{M_n}$ for LPELA macromonomers as a function of the feed lactide to PEG (LEGF) molar feed ratio is summarized in Table 1. LEGF ratio was varied from zero to 20 intervals of 5. The nL values, changed from 0 to 3.6, 7.4, 9.6 and 14.8 for LPELA as LEGF was increased from zero to 5, 10, 15, and 20, respectively. <1.5. As

LEGF ratio was increased from zero to 20, the $\overline{M_n}$ of of LPELA increased from 4.7 to 6.8 kDa. As LEGF ratio was increased from zero to 20, the number of lactides per arm of macromonomer increased from zero to 7.4 for LPELA. The range for acrylate fraction per arm of LPELA macromonomers was 0.71-0.89. . In general, polydispersity of SPELA and LPELA macromonomers was <1.5.

Macromonomer	$\overline{M}_n$ (±100)	Monomer/PEG feed molar ratio	Number average of monomer units per end group (±0.1)	Number average of acrylate group per end group (±0.05)
SPEXA-nX0	5300	0	0	0.85
SPECA-nC2.8	5500	5	0.7	0.85
SPECA-nC4.8	5700	7.5	1.2	0.81
SPECA-nC7.2	6000	10	1.8	0.78
SPECA-nC11.2	6400	15	2.8	0.75
SPEDA-nD2.4	5400	5	0.6	0.82
SPEDA-nD4.4	5600	7.5	1.1	0.79
SPEDA-nD6.8	5900	10	1.7	0.75
SPEDA-nD11.6	6300	15	2.9	0.73
SPEGA-nG2.4	5600	5	0.8	0.87
SPEGA-nG4.4	5700	7.5	1.2	0.82
SPEGA-nG6.4	5900	10	1.6	0.81
SPEGA-nG11.2	6500	15	2.8	0.78
SPELA-nL3.2	5700	5	0.8	0.86
SPELA-nL4.4	5800	7.5	1.1	0.83
SPELA-nL6.4	6200	10	1.6	0.82
SPELA-nL11.6	6900	15	2.9	0.74
LPELA-nL3.6	5200	5	1.8	0.85
LPELA-nL7.4	5800	10	3.7	0.87
LPELA-nL9.6	6100	15	4.8	0.77
LPELA-nL14.8	6800	20	7.4	0.71

Table 1: Number of degradable monomers per macromonomer (nC,nD, nG and nL), number-average molecular weight ($\overline{M}_n$) average number of lactide units per end group, and average number of acrylate groups per end group for SPECA, SPEDA, SPEGA, SPELA and LPELA macromonomers as a function of monomer to PEG molar feed ratio in the polymerization reaction.

4.2 Effect of Initiator on Gelation Kinetics

The effect of initiator concentration on the storage modulus and gelation time of the LPELA-nL7.4 and SPELA-nL14.8 macromonomers (both having 3.7 lactide

monomers per end group) is shown in Figure 8a and 8b, respectively. It is well established that the viability of cells encapsulated in synthetic gels is adversely affected by low molecular weight species such as initiators, crosslinkers, and small-molecule monomers that cross the cell membrane. Based on previous studies, photoinitiator concentrations >2 wt% (based on the weight of macromonomer) significantly decreased the viability of the seeded cells. Therefore, the effect of initiator on gelation of SPELA and LPELA was tested with concentrations <1.4 wt%. For each initiator concentration, The modulus of SPELA gel was significantly higher than that of LPELA. The modulus of the hydrogels showed a maximum at 0.38 wt% initiator concentration for both LPELA-nL7.4 and SPELA-nL14.8 macromonomers. As the initiator concentration was increased from 0.08 to 0.38 wt%, the modulus of LPELA and SPELA gels initially increased from 13.1 ± 3.0 to 20.2 ± 4.1 kPa and from 17.5 ± 2.0 to 37.5 ± 2.5 kPa, respectively. After that, the modulus decreased to 17.2 ± 2.1 and 32.9 ± 2.5 kPa for LPELA and SPELA hydrogels, respectively, when the initiator concentration was increased to 1.31 wt%. The modulus of the gels did not change for initiator concentrations >0.8 wt%. The initial increase in the gel modulus with initiator concentration can be attributed to an increase in the propagation rate (R_p) given by:

$$R_P = K_P [AC] \left[\frac{R_i}{K_t} \right]^{1/2} \qquad (20)$$

$$R_i = \phi \varepsilon I_0 \delta [I] \qquad (21)$$

where K_P and K_t are the rate constants for chain propagation and termination respectively, R_i is the radical initiation rate, [AC] is the concentration of unreacted acrylates, ϕ is initiation efficiency, ε is molar extinction coefficient, I_0 is the intensity

of incident radiation, δ is sample thickness, and $[I]$ is photoinitiator concentration. According to equation 12, the rate of radical production increased with increasing the initiator concentration to 0.38 wt% leading to a higher propagation rate of acrylates and higher extent of crosslinking. For initiator concentrations exceeding 0.38 wt%, the probability of formation of more than one radical on the same macromonomer increased, which lead to the formation intra-molecular crosslinking, as opposed to inter-molecular crosslinking, and cluster formation and a decrease in storage modulus.[27] For initiator concentrations >0.8 wt%, the increase in propagation rate was offset by the increase in the rate of intra-molecular crosslinking, resulting in no change in modulus with increase in initiator concentration.

The gelation time of LPELA and SPELA macromonomers as a function of initiator concentration is shown in Figure 8b. As the initiator concentration was increased from 0.08 to 0.78 wt%, gelation time of LPELA and SPELA macromonomers decreased from 140 ± 5 to 45 ± 1 s and from 200 ± 9 to 42 ± 2 s, respectively. At low initiator concentrations (0.08 to 0.23 wt%), SPELA had higher gelation times than LPELA but the two macromonomers reached similar gelation times for concentrations >0.5 wt%. As described in the following paragraph, the total volume of the hydrophobic micelles in SPELA-nL14.8 is higher than LPELA-nL7.4. As a result, at low initiator concentrations, it is more likely for the polymerization reaction in SPELA to become diffusion controlled than LPELA, leading to a higher gelation time for SPELA. As the initiator concentration is increased above 0.23 wt%, the reaction becomes less controlled by diffusion, leading to comparable gelation times for LPELA and SPELA at higher concentrations. In addition, the higher concentration of reactive acrylates in SPELA is offset by the higher probability

of intra-molecular crosslinking, leading to comparable gelation times for SPELA and LPELA at initiator concentrations >0.23 wt%. In the experiments that follow, the initiator concentration of 0.75 wt% is used, unless otherwise specified, to have low gelation time as well as high shear storage modulus.

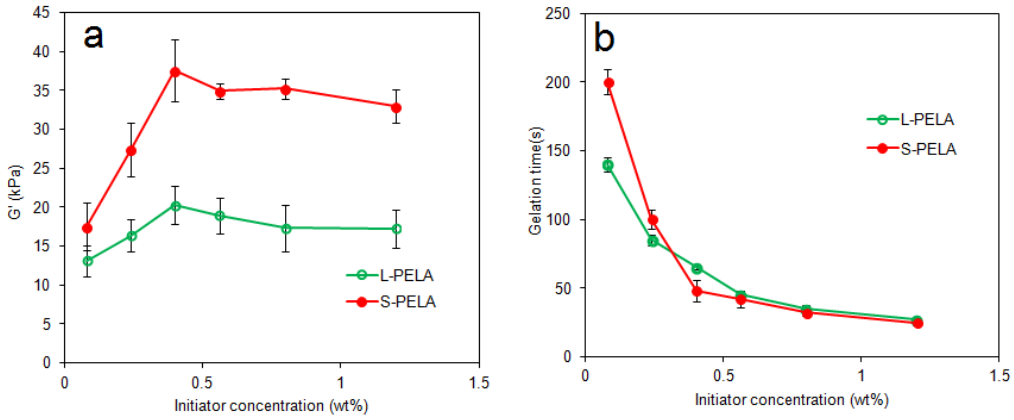

Figure 8: Effect of UV initiator concentration on (a) storage modulus and (b) gelation time of LPELA-nL7.4-M20 and SPELA-nL14.8-M20 hydrogels. Error bars correspond to means ± 1 SD for n = 3.

4.3 Effect of Acrylate Group Concentration on Gelation Kinetics

The effect of acrylate group concentration in the precursor solution on compressive modulus, gelation time, swelling ratio and sol fraction of SPECA-7.2nC, SPEDA-6.8nD, SPEGA-6.4nG and SPELA-6.4nL (corresponding to XEGF ratio of 10) hydrogels have been shown in Figures 9a, b, c and d, respectively. As the acrylate group concentration increases from 0.05 to 0.13 mol/lit, the compressive modulus of SPEXA hydrogels increase from 46 to 484 kPa, 39 to 559 kPa, 51 to 710 and 20 to 456 kPa for X=C,D,G and L, respectively.

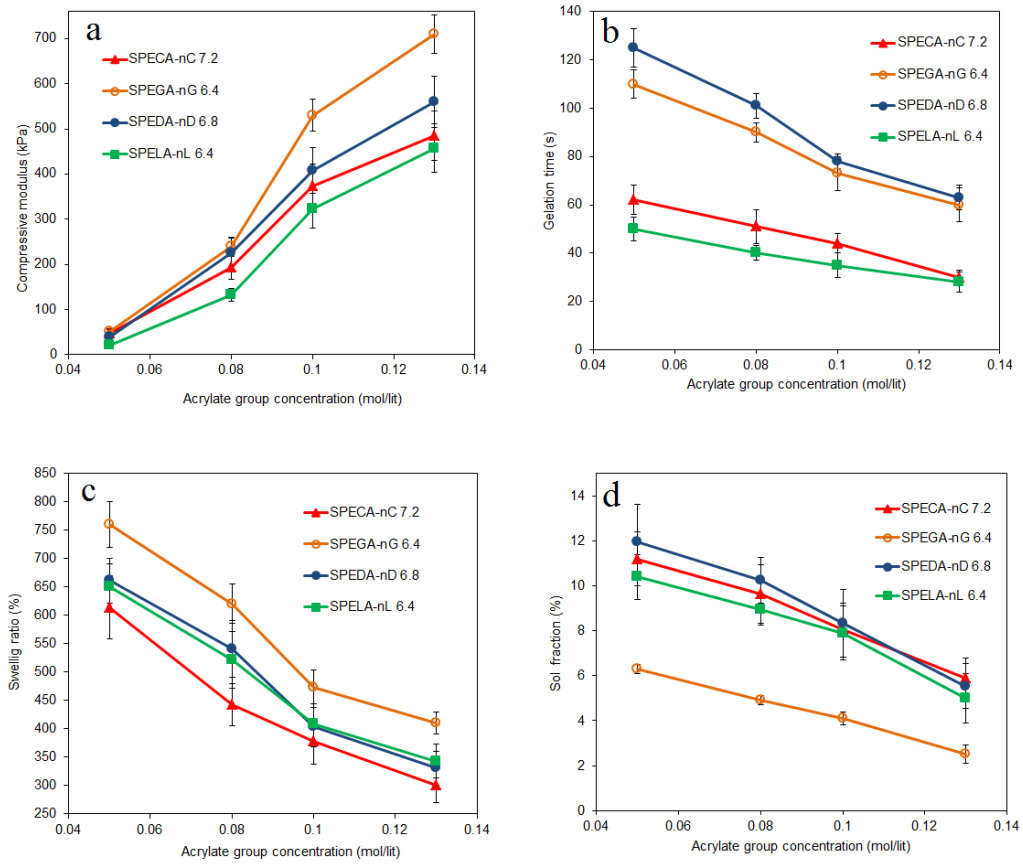

Figure 9: Effect of acrylate group concentration on (a) compressive modulus and (b) gelation time c) swelling ratio and d) sol faction of SPECA-nC7.2, SPEDA-nD6.8, SPEGA-nG6.4 and SPELA-nL6.4 hydrogels. Error bars correspond to means ± 1 SD for n = 3.

The gelation time of SPEDA and SPEGA hydrogels had no significant difference and changed from 125 to 63s and 110 to 60s, respectively, which was longer than that of SPECA and SPELA gels changing from 62 to 30s and 50 to 28s, respectively, when the acrylate group concentration increases from 0.05 to 0.13 mol/lit. The swelling ratio of SPECA decreased from 613 to 300 as the acrylate group concentration changed from 0.05 to 0.1mol/lit .The swelling ratio of SPEDA and SPELA gels showed similar behavior and decreased from 660 to 338% by changing the acrylate group concentration from 0.05 to 0.1mol/lit. SPEGA gel demonstrated more hydrophilic nature with the

swelling ratio value decreasing from 760 to 433% as the acrylate concentration increases from 0.05 to 0.1mol/lit.

The sol fraction of SPECA, SPEDA and SPELA gels had similar values and changed from 11 to 6%, 12 to 5.5% and 10 to 5%, respectively, as the acrylate group concentration changed from 0.05 to 0.13 mol/lit. SPEGA gels showed the lowest sol fraction at each point varying from 6.5 to 2.5% by changing the acrylate concentration from 0.05 to 0.13 mol/lit.

4.4 Effect of Number of Monomer Per End Group of the Macromonomer on Gelation Kinetics

The effect of the number of monomers per end group of the macromonomer at an acrylate group concentration of 0.1 mol/lit (SPEXA-A10) on compressive modulus, gelation time, swelling ratio and sol faction of SPECA-A10, SPEDA-A10, SPEGA-A10 and SPELA-A10 hydrogels has been shown in Figures 10 a, b, c and d, respectively. SPELA-A10's compressive modulus, which was the lowest among all the moacromonomers, showed a slight increase (from 330 to 390 kPa) when the number of lactide molecules increased from 0 to 2.9 on each chain. The compressive modulus of SPECA-A10 did not have a significant change (from 330 to 373kPa) as nC varied from 0 to 1.8, respectively. Afterward, E increased with a higher rate to 424 kPa when nC increased to 2.8. No significant change was observed in the compressive modulus of SPEDA-A10 and SPEGA-A10 (from 330 to 324 and from 330 to 336 kPa, respectively) as the number of monomers per end group of the macromonomer was varied from 0 to 0.7. However, it changed with an increasing trend to 530 and 625 kPa, respectively, by increasing the nX up to 2.9. Also, it is obvious that SPEGA-A10 has the highest and SPELA-A10 has the lowest modulus at each specific number of monomer. SPEDA-A10

and SPEGA-A10 demonstrated longer gelation times compared to SPECA-A10 and SPELA-A10. As the number of monomers per end group of the macromonomer increased from 0 to 2.9, the gelation time of the SPEDA-A10 and SPEGA-A10 decreased from 150 to 64 and 61s, respectively, while that of to SPECA-A10 and SPELA-A10 decreased from 150 to 34 and 38s, respectively. The swelling ratio of all four types of macromonomers had a decreasing tendency by increasing nX and SPEGA-A10 indicated the highest swelling ratio while SPECA-A10 indicated the lowest one. The swelling ratio of SPECA-A10, SPELA-A10, SPEDA-A10 and SPEGA-A10 hydrogels decreased from 490 to 350, 385, 370 and 430 %, respectively, by increasing the nX from 0 to 2.9. As it is observed in Figure 10 d, SPEGA-A10 exhibits the lowest sol fraction and there is no appreciable difference among that of the other macromonomers. The sol fraction of SPECA-A10, SPELA-A10, and SPEDA-A10 changed from 9.56 to 6.36, 6.26 and 7.24%, respectively, while that of SPEGA-A10 changed from 9.56 to 3.1% when nX varied from 0 to 2.9.

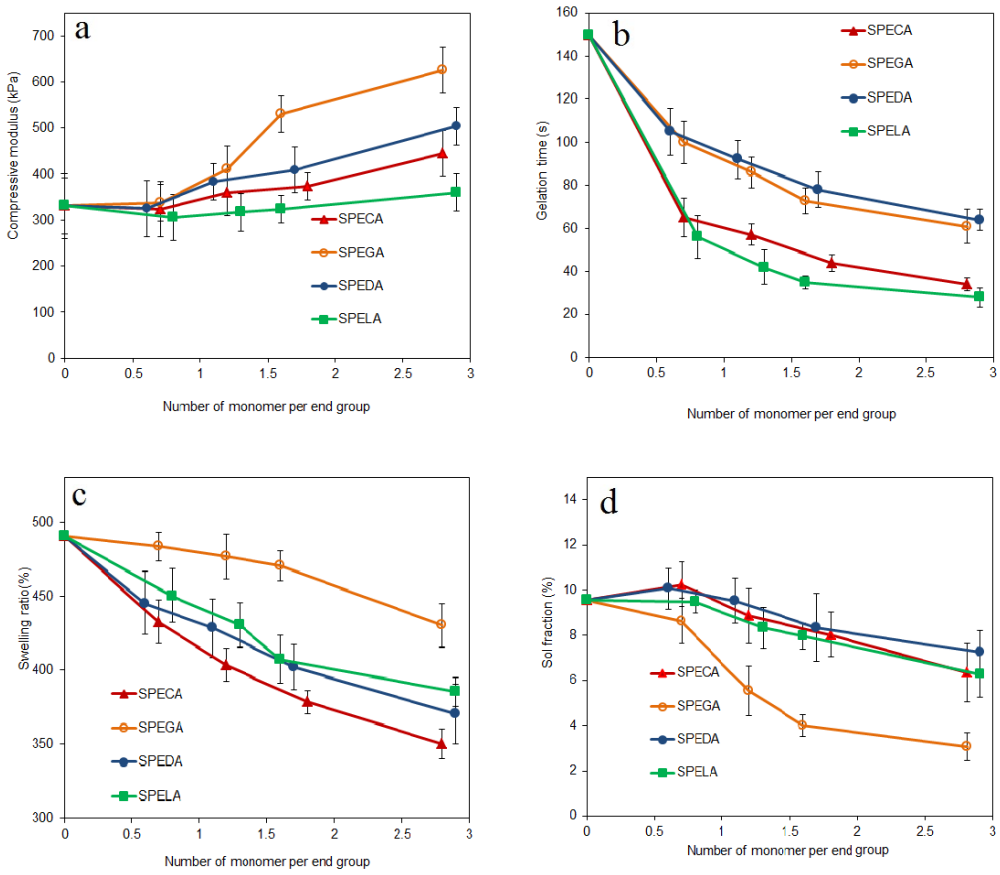

Figure 10: Effect of number of monomer per end group on (a) compressive modulus and (b) gelation time c) swelling ratio and d) sol faction of SPECA-A10, SPEDA-A10, SPEGA-A10 and SPELA-A10 hydrogels. Error bars correspond to means ± 1 SD for n = 3.

4.5 Effect of Monomer Type on Macromonomer Degradation

The effect of monomer type on the mass remaining of SPECA-7.2nC, SPEDA-6.8nD, and SPEGA-6.4nG and SPELA-6.4nL hydrogels has been shown in Figure 11. As it is observed, SPEGA-6.4nG had the fastest degradation rate among all types of the hydrogels with mass loss of 100% in less than 3 days. The mass loss of SPELA-6.4nL, which was slower than SPEGA, was more than 94% after 35 days. The slowest degradation rates were demonstrated by SPECA-7.2nC and SPEDA-6.8nD with mass loss of 19 and 39%, respectively, after 40 days.

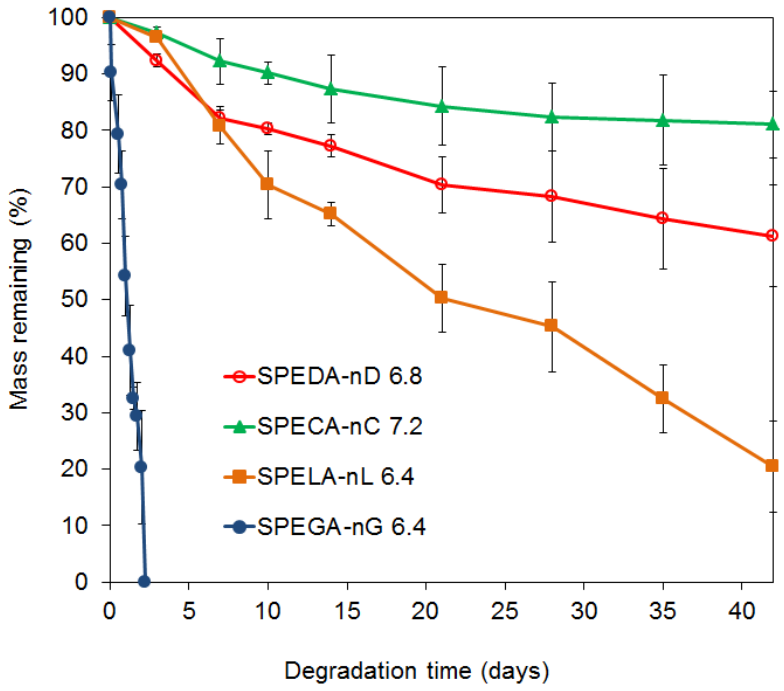

Figure 11: Mass remaining of SPECA-nC7.2-A10, SPEDA-nD6.8-A10, SPEGA-nG6.4-A10 and SPELA-nL6.4-A10 hydrogels with incubation time. Error bars correspond to means ± 1 SD for n = 3.

4.6 Effect of Number of Monomer Per End Group of the Macromonomer on Degradation

Figures 12 a, b, c, and d show the impact of number of monomer per end group of the macromonomer on degradation rate of SPECA-A10, SPEDA-A10, SPEGA-A10 and SPELA-A10 hydrogels, respectively. The degradation rate of SPECA hydrogels showed no significant difference between nC= 2.8 and 4.8 as was the same for nC=7.2 and 11.2. The mass losses of SPECA-A10 hydrogels changed from 11% to 12, 18.1 and 18.4% as the number of Caprolactone molecules per end group of the macromonomer increased from 2.8 to 4.8, 7.2 and 11.2, respectively, after 42 days. SPEDA based hydrogels showed a similar degradation trend and no appreciable difference was observed among

all of the groups. After 42 days, the SPEDA hydrogels had mass losses of 30, 35, 38, and 34% when nD varied from 2.4 to 4.4, 6.8, and 11.6, respectively.

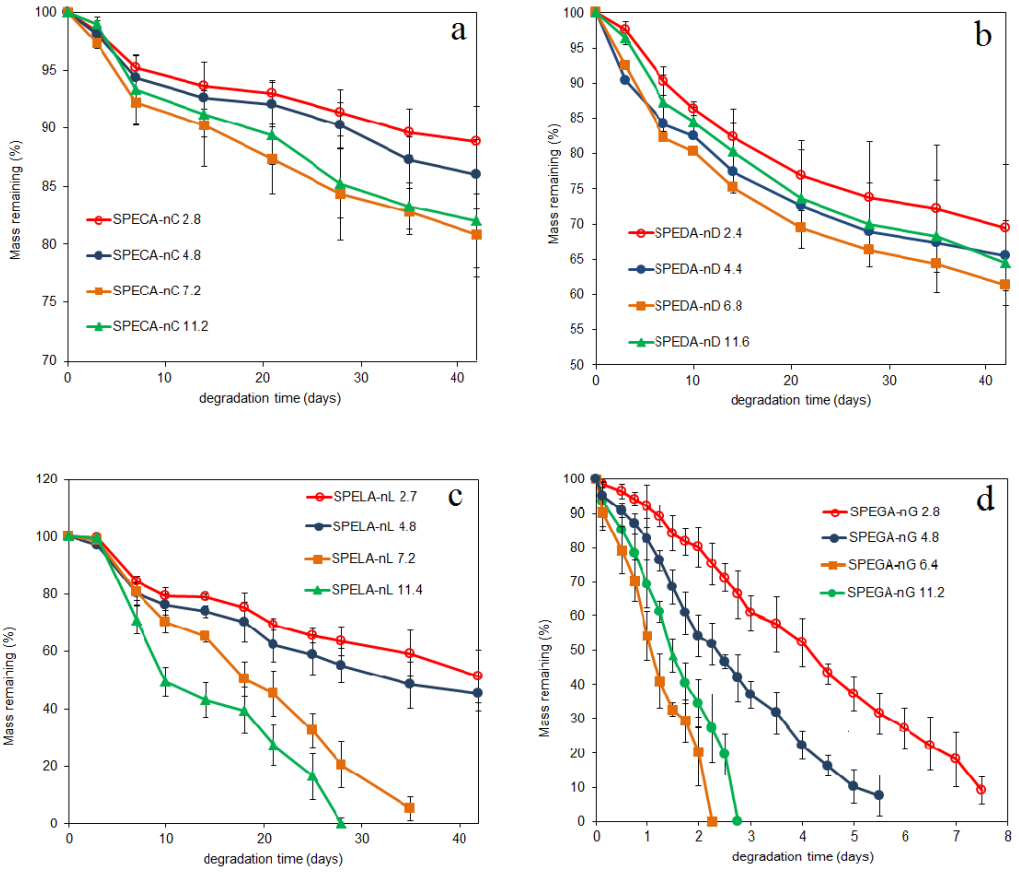

Figure 12: Mass remaining of SPECA (a), SPEDA (b), SPEGA (c) and SPELA (d) hydrogels in different number of monomers per end group of the macromonomer with incubation time. Error bars correspond to means ± 1 SD for n = 3.

The degradation rate of SPELA hydrogels increased by increasing the number of Lactide molecules per end group of the macromonomer . The mass loss of the SPELA-nL7.2 hydrogel was 95% and that of the SPELA-nL 11.4 hydrogel was 100% after 35 and 28 days, respectively. Also, the mass loss of SPELA-nL2.7 and SPELA-nL4.8 was 55 and 49%, respectively, after 42 days. SPEGA based hydrogels exhibited much faster

degradation rates than the other types of hydrogels. For example, the slowest of them, SPEGA-nG 2.8, was degraded completely after less than 10 days. Also, they showed a biphasical behavior. SPEGA 6.4, with 100% mass loss after 2.5 days, degraded faster than SPEGA 4.8 and SPEGA 11.2, which reached 100% mass loss after 6 and 2.75 days, respectively.

4.7 Swelling Ratio Variation By Incubation Time

Figures 13 a, b, c, and d show the effect of number of monomer per end group of the macromonomer on swelling ratio variation of SPECA-A10, SPEDA-A10, SPEGA-A10 and SPELA-A10 hydrogels, respectively, by degradation time. The swelling of SPECA hydrogels showed no significant difference between nC= 2.8 and 4.8 and also between nC=7.2 and 11.2. The swelling ratios of SPECA-A10 hydrogels changed from 410% to 463, 378 to 453%, 350 to 402% and 320 to 375% as the number of Caprolactone molecules per end group of the macromonomer increased from 2.8 to 4.8, 7.2 and 11.2, respectively, after 42 days. The SPEDA based hydrogels' swelling ratio increased from 441% to 565, 416 to 543%, 435 to 538% and 394 to 516% when nD varied from 2.4 to 4.4, 6.8, and 11.6, respectively. No appreciable difference was observed among all of the SPEDA gels group groups. The increasing rate of SPELA hydrogels' swelling ratio by degradation time was different for various numbers of Lactide molecules per end group of the macromonomer. The swelling ratio of the SPELA-nL7.2 hydrogel increased from 383 to 670% and that of the SPELA-nL 11.4 hydrogel increased from 363 to 660% after 21 and 14 days, respectively. The swelling ratio measurement of these hydrogels could not be done further because the samples were too loose. Also, the swelling ratio of SPELA-nL2.7 and SPELA-nL4.8 changed from 406 to 652% and 391 to 710%, respectively, after 42 days.

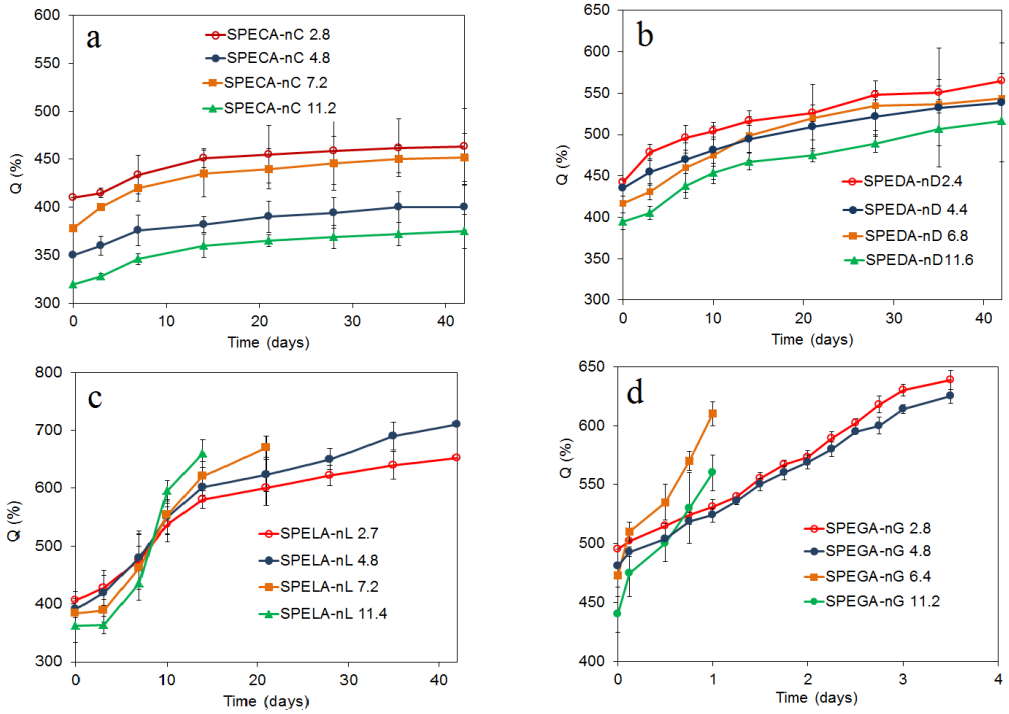

Figure 13: Swelling ratio of SPECA (a), SPEDA (b), SPEGA (c) and SPELA (d) hydrogels in different number of monomers per end group of the macromonomer with incubation time. Error bars correspond to means ± 1 SD for n = 3.

The swelling ratio of SPEGA-nG6.4 and SPEGA-nG11.2 increased from 473 to 610% and 440 to 560%, respectively, after one day. Also, that of SPEGA-nG2.8 nd SPEGA-nG4.8 changed from 495 to 639% and 481 to 625 %, respectively, after 3.5 days.

4.8 Effect of Different Monomers on Cell Viability and Osteogenic Differentiation

Images a−d in Figure 14 show live (green) and dead (red) cells 1 h after encapsulation in SPEXA-nX0 (a) SPECA-nC7.2 (b), SPEDA-nD6.8 (c) and SPELA-nL6 (d) hydrogels, respectively. According to the live-dead staining images, the different macromonemers,

which have constant compressive modulus but different degradation profile did not have a significant effect on cell viability. Cell viability was quantitatively analyzed by counting the number of live and dead cells. The fraction of viable cells for SPEXA-nX0 (a), SPECA-nC7.2 (b), SPEDA-nD6.8 (c) and SPELA-nL6 (d) hydrogels was 89 ± 4, 91 ± 2, 91 ± 3, and 92 ± 4, respectively. DNA content, extent of mineralization, and the total collagen content of MSCs encapsulated in SPEXA gels are shown in

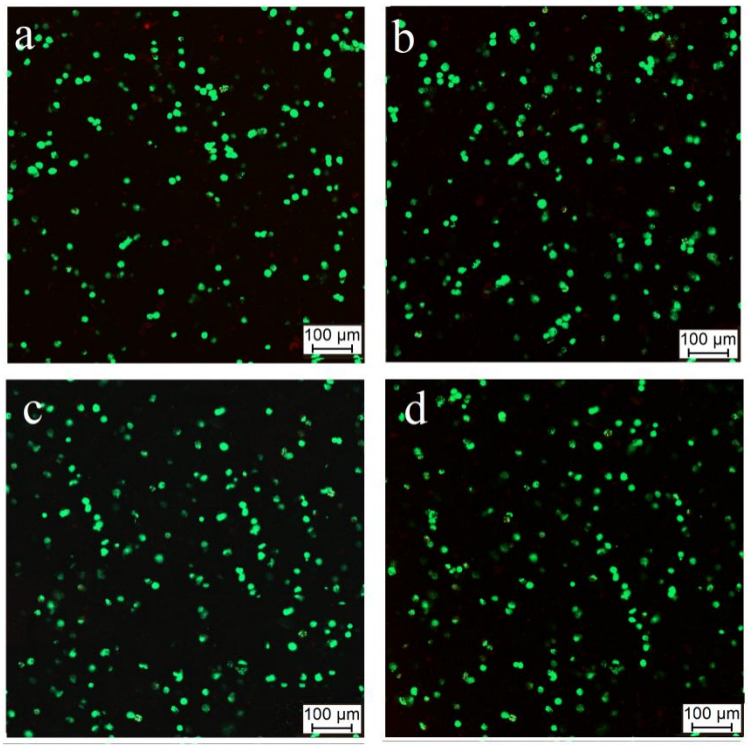

Figure 14: Live (green) and dead (red) image of MSCs 1 h after encapsulation in SPEXA-nX0 (a) SPECA-nC7.2 (b), SPEDA-nD6.8 (c) and SPELA-nL6.4 (d).

Figure 15 a−c, respectively. At day 14 and 28, DNA content of MSCs in all the groups decreased slightly compared with day 7. For day 28, DNA content of MSCs in

SPELA gels was significantly lower than SPEXA-nX0 gels (indicated by a star in Figure 15a). Calcium content of SPEXA gels increased significantly on days 14 and 28 compared with day 7. At day 28, calcium content of the SPELA group was significantly higher than SPEXA-nX0 (control) (indicated by one star), and SPECA and SPEDA groups (indicated by two stars). However, there is no significance difference SPECA, and SPEDA groups compared to SPEXA-nX0 (control). For example, calcium contents of the SPELA group after 28 days was 224.7 ± 18.4 mg Ca/mg DNA, respectively, whereas those of SPECA, SPEDA, and SPEXA-nX0 were 159.6 ± 19.9, 150.8 ± 16.8, and 99.6 ± 29.2 mg Ca/mg DNA.

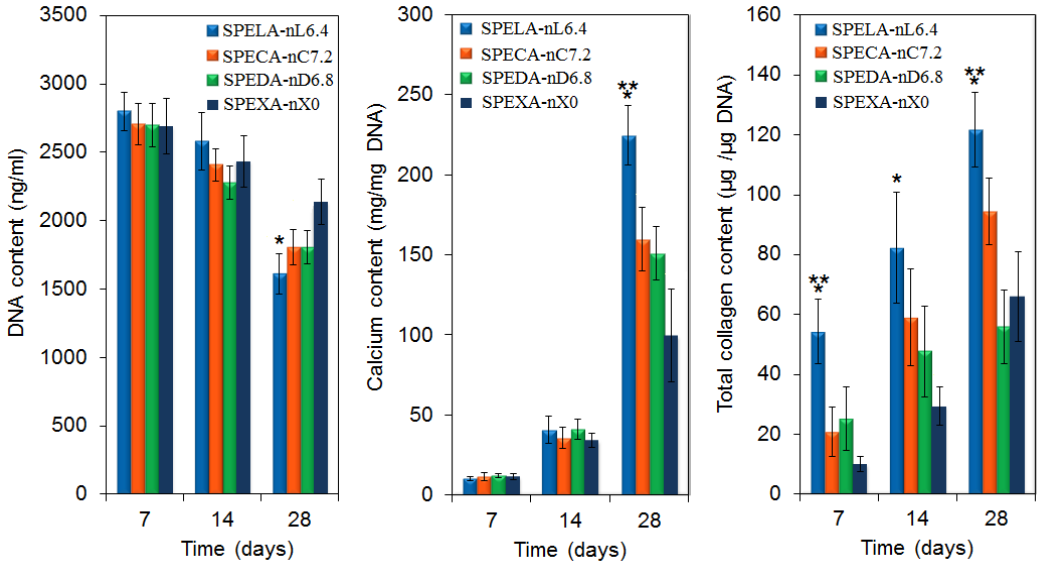

Figure 15: DNA content (a) and calcium content (c) and total collagen amount (d) of differentiating BMS cells as a function of incubation time encapsulated into SPEXA-nX0, SPECA-nC7.2, SPEDA-nD6.8 and SPELA-nL6.4 hydrogels cultured in osteogenic media.

"*" indicates significant difference between SPEXA-nX 0(control) and the other hydrogels at the same time point.

"**" indicates significant difference between SPELA-nL6.4 and the other hydrogels at the same time poin.

The total collagen content results showed consistency with the Ca content results. At

day 7 and 28, SPELA gels had significantly higher collagen content compared to SPEXA-nX0, SPECA, and SPEDA. For instance, collagen content in SPELA gels after 7 and 28 days were, 54.3 ± 10.9 and 121.8 ± 12.6 µg Collagen/µg DNA, respectively, whereas those of SPEXA-nX0, SPECA, and SPEDA were 20.9 ± 8.4, 94.4 ± 11.1, 25.3 ± 10.5, 55.9 ± 12.2, and 10 ± 2.6, 65.9 ± 15.

5 . Discussion

The properties of hydrogels have been shown to be very dependent on concentration of the reactive groups as it is observed at Figure 9. Eq. 22 shows the dependency of the propagation rate of photopolymerization reaction on acrylate group concentrationrate of photopolymerization reaction on acrylate group concentration [42.48]:

$$R_P = K_P[AC]\left[\frac{R_i}{K_t}\right]^{1/2} \qquad (22)$$

$$R_i = \phi \varepsilon I_0 \delta[I] \qquad (23)$$

where K_p and K_t are the rate constants for chain propagation and termination respectively, R_i is the radical initiation rate, [AC] is the concentration of unreacted acrylates, ϕ is initiation efficiency, ε is molar extinction coefficient, I_0 is the intensity of incident radiation, δ is sample thickness, and [I] is photoinitiator concentration. According to this equation, higher concentration of acrylate groups leads to higher crosslinking density, higher propagation rate and consequently shorter gelation time for all types of the macromonomers. In addition, Eq. 24 represents the shear modulus of an ideal network is proportional to the density of elastically active links according to the theory of rubber elasticity [42.48]:

$$G = \nu_E RT \qquad (24)$$

where v_E is a molar concentration of elastically effective chains (EEC), R is the gas constant, and T is the absolute temperature. Therefore, the higher acrylate group concentration of the macromonomers results in higher density of elastically active chains, and consequently higher modulus. Since intermolecular reactions lead to forming branched structures, it is acceptable to assume that these SPEXA hydrogels contain cross-linked clusters embedded in a solution-like matrix. As the concentration increases, the probability of intra-molecular crosslinks, which cause loop formation and unreacted pendant double bonds, decrease. Hence, macromonomer solution becomes more ideal to form uniformly dispersed clusters, thereby contributing to the formation of a stronger network and lower sol fraction. In addition, the decreasing trend of the macromonomers swelling ratio by increasing the acrylate group concentration can be attributed to the dependency of crosslinking density and mesh size of the networks to the reactive group concentration. The higher modulus exhibits higher crosslinking density, smaller mesh size and consequently lower swelling ratio.

Macroscopic liquid-liquid phase separation due to the attractive hydrophobic interaction is considered as a new gelation mechanism apart from the conventional gelation due to the micelle packing. Using this concept, the increasing trend of the compressive modulus of SPEXA hydrogels by increasing the monomer segment length, showed in Figure 10 a, can be explained. Since the C, D, G and L are all hydrophobic units, with different degrees of hydrophobicity; the chain ends of the macromonomers tend to aggregate and form micelles due to the hydrophobic interactions. This mechanism of micelle formation which leads to the localization of acrylate groups in the micelles core, decreases the average distance and enhances the probability of the interaction

between the reactive groups. Consequently, the conversion of photopolymerization reaction is raised resulting in the higher modulus and crosslinking density. When the number of monomers is increased to the higher values, the number-average micelle core radius is increased and the initial micellar structure are found to be disrupted and micelle clusters are formed due to the more intensive attractive hydrophobic interaction between the core phases. As a result, the gelation time is decreased by forming more closely packed micelles while the modulus is increased (Figures. 10 a and b). Besides, increasing the monomer length (hydrophobic segment) enriches the hydrophobicity of the whole macromonmer. As the increasing trend of crosslinking density and hydrophobicity both have negative effects on swelling ratio, the swelling ratio of all the SPEXA hydrogels decrease by increasing the number of monomer per end groups of the macromonomer (Figure 10 c). Furthermore, the higher density of reactive acrylate groups in higher amount of hydrophobic segments, which increased the probability of incorporating macromonomers in the gel network, leads to the decreasing trend of sol fraction when the monomer length increases (Figure 10 d).

Moreover, as it is observed in Figures. 9 a and 10 a, SPEGA hydrogels have the highest modulus among all types of the hydorgels at each specific acrylate group concentration and monomer length. When the glycolide units are replaced by more hydrophobic segments (D, C and L), due to increasing the hydrophobicity of the micelles core and then lower water content of the micelles, the mobility of the acrylate groups and diffusion of the initiator in the micelles significantly decreased. Besides, more hydrophobic units in the macromonomer structure cause the gel formation not by the ordered state through the micellar packing but by the random aggregation of the micelles.

These factors lead to highest modulus and lowest sol fraction of SPEGA hydrogel [52.60]. Also, due to the presence of the ether bonds (CH-O-CH) in dioxanone units (Figure 6), SEPDA macromoonmer contains more hydrophilic and flexible chains compared to SPECA and SPELA resulting in formation of the hydrogels with higher modulus. In addition, the higher tendency to aggregation due to the presence of more hydrophobic units in SPECA and SPELA decreased the average distance between the acrylate groups, causing lower gelation time for these hydrogels compared to SPEDA and SPEGA based hydrogels (Figures 9 b and 10 b). As it was mentioned, both higher crosslinking density and hydrophobicity decrease the swelling ratio of the resulting hydrogel. Therefore, the swelling ratio of SPECA hydrogels is the lowest among all four types of hydrogels.

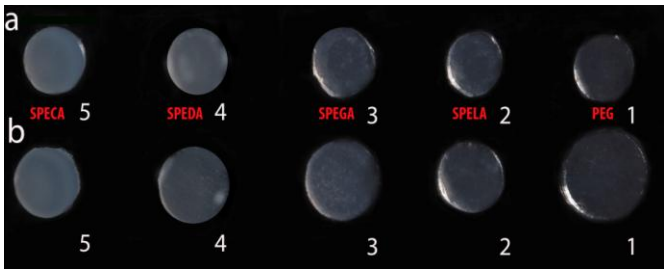

Figure 16: . SPEXA (1. PEG, 2. SEPLA, 3. SPEGA, 4. SPEDA and 5. SPECA) based hydrogels (a) before and (b) after swelling at a concentration of 15 wt%.

As it was explained, the modulus (consequently crosslinking density) of the SPEDA hydrogel is higher than that of SPELA while SPELA chains are more hydrophobic than SPEDA ones. Because of that, they exhibit similar trend in swelling ratio with no significant difference. Furthermore, SPEGA based hydrogels have the highest swelling ratio as the most hydrophilic macromonomer.

Varying the monomer type and the ratio of the degradable segments in the macromonomer structure are two important strategies to control the degradation rate of

the hydrogels as it has been shown in Figures 11 and 12. The hydrolysis rate of the SPEXA based hydrogels can be evaluated by the following equation [42.48]:

$$R_{\deg,SPELA} = k[-COO-][H_2O] \quad (6)$$

Where k is the degradation rate constant, and [-COO-] and [H_2O] are the concentrations of ester groups and water in the hydrogel, respectively. Based on this equation the rate of hydrolysis is proportional to the water content of the swollen network and number of hydrolysable groups. As the hydrogels degrade, the water content increase and consequently further promotes the rate of hydrolysis. On the other hand, the concentration of the carboxylic groups, which are responsible for the degradation, decreases by degradation of the hydrogels. As a result, these effects work together to create a nearly constant degradation rate, as can be seen in Figure 11. Moreover, increasing the degradable segment length leads to the higher concentration of the carboxylic group. However, increasing the number of methylene groups (degradable segment length) effectively increases the hydrophobicity of the group adjacent to the ester, crosslinking density and crystallinity of the network making it less accessible to water and consequently reducing the degradation rate. Hence, the increase in the mass loss of SPEGA and SPELA hydrogels by increasing the nG and nL up to 6.8 and 11.4, respectively, can be attributed to the higher concentration of ester groups of the hydrogels. The decrease in mass loss for nG>6.8 is attributed to micelle formation with significantly reduced local concentration of water, leading to reduced rate of degradation. The same behavior was observed for SPELA for nL>11.4 as shown in our previous publication. It should be mentioned that in the case of SPEDA and SPECA hydrogels, one ester group (responsible for degradation) is added to the chain based on adding one

repeating unit of the monomer (C and D) while that of SPEGA and SPELA is two (G and L). Because of that, the sensitivity of degradation rate to the number of monomer in SPECA and SPEDA are lower than SPELA and SPEGA hydrogels. In addition, the five methylene groups in a C unit [C = $COO(CH_2)_5$] make the SPECA chain unit more hydrophobic (least swelling ratio) than other macromonomers' (L, D and G). As a result, the hydrolysis rate of SPECA hydrogel is slowest among all four types of hydrogels while SPEGA based hydrogels showed the fastest degradation rate because of the higher concentration of the ester groups and highest swelling ratio (Figure 12).

It is widely considered that cells sense the stiffness of the hydrogels and they function most physiologically when the stiffness of the underlying hydrogel is optimum for the particular lineage [35.36]. Engler et al. reported that when hBMSCs cultured on 25 kPa-40 kPa modulus range polyacrylamide gels demonstrated increased expression of osteogenic markers compared to when hBMSCs cultured in 8 kPa-15 kPa range gels . In addition, Parekh et al. investigated the effect of hydrogel modulus on stem cell differentiation in 3D photopolymerized poly(ethylene glycol) (PEG)-based hydrogels. It was shown that hBMSCs had significantly higher osteogenic differentiation capacity when they were cultured in 59 kPa hydrogels compared to 0.5 and 11 kPa hydrogels . Therefore, in these study concentrations corresponding to 50 kPa modulus for SPEXA-nX0 (a) SPECA-nC7.2 (b), SPEDA-nD6.8 (c) and SPELA-nL6 were selected for encapsulation and osteogenic differentiation. Since the degradation rate is relatively high in SPEGA hydrogels (<7days), cell encapsulation and osteogenic differentiation could not be conducted.

DNA content of MSCs in the SPEXA gels decreased slightly with the incubation

time. This trend is consistent with previous reports that cell number decreases with differentiation of MSCs in osteogenic medium. Wang et al. reported a decrease of 24 and 51% in DNA content after 3 and 6 weeks, respectively, with osteogenic differentiation of human umbilical cord MSCs seeded in PLGA scaffolds . Moreover, Oliveira et al. demonstrated a decrease of 20% in DNA content after 7−14 days with osteogenic differentiation of rat MSCs. The higher calcium and collagen content in SPELA gels compared to SPEXA-nX0 (control), SPECA, and SPEDA gels may be related to the faster degradable nature of SPELA matrix, leading to increase in water content, free volume, and greater cell-matrix interaction with incubation time. Therefore, as the gel degrades the cells need to produce more matrixes in order to maintain attached to an extracellular supporting environment. Due to the lower degradation rates of SPECA, and SPEDA, there is no significantly difference on calcium and collagen content among SPECA, SPEDA, and SPEXA-nX0 (control) gels. These results were consistent with Nuttelman et al. where they reported significantly higher extends of mineralization when they encapsulated hMSC in degradable PEG hydrogels compared to non-degradable PEG hydrogels as a control. In addition, Benoit et al. demonstrated that mineralization of osteoblasts increased 3 fold with increasing the degradation rate of poly(ethylene glycol) dimethacrylate **.** The higher production of collagen in the higher degradable SPELA gels might be related to prevent the structural collapse of the hydrogel by replacing it with bone extracellular matrix [62.65].

As shown in Figure 5b, the shear modulus of SPELA gels was significantly higher than those of LPELA for all macromonomer concentrations. For example, the ratio of increased from 1.2 at 10 wt% macromonomer concentration to 2.2 at 25 wt%. As

mentioned in the last paragraph, the lower values of at the low concentrations can be attributed to the macromonomer architecture and its effect on nano-scale structure formation. Previous DPD simulation of the macromonomers in aqueous solution showed localization of reactive Ac beads, due to aggregation and micelle formation by the hydrophobic lactide (L) beads. The localization of Ac beads leads to the formation of elastically active inter-molecular and elastically inactive intra-molecular crosslinks. The higher acrylate densities for SPELA compared to LPELA and higher macromonomer concentrations led to higher propagation rates, higher density of elastically active chains, and higher modulus. Furthermore, due to a larger average distance between the macromonomers at low concentrations, the probability of intra-molecular crosslinks that lead to loop formation and cyclization is higher.36 Since intra-molecular crosslinks are not elastically active and do not contribute to the modulus of the network, the higher density of acrylates in SPELA is offset by higher intra-molecular crosslinks, leading to a smaller difference between the modulus of SPELA and LPELA gels at low concentrations (see Figure 5b). As the macromonomer concentration is increased, the probability of intra-molecular links decreases, 51 leading the higher fraction of elastically active crosslinks in SPELA and larger difference between the moduli of SPELA and LPELA.

6 . Conclusion

A novel approach to tissue regeneration is to encapsulate progenitor cells in inert, non-fouling, biodegradable hydrogels loaded with soluble growth factors to guide their differentiation and maturation. This approach allows the cells to secret the desired matrix in an inert microenvironment. To this end, linear (LPELA) and star (SPELA) poly(ethylene glycol-co-lactide), star (SPECA) poly(ethylene glycol-co-caprolactone), star (SPEDA) poly(ethylene glycol-co-dioxanone), star (SPEGA) poly(ethylene glycol-co-glyclide), acrylate macromonomers with short biodegradable segments were synthesized and characterized with respect to modulus, gelation time, sol fraction, water content, and degradation. SPELA hydrogels had significantly higher modulus, lower gelation time, and lower sol fraction in comparison with linear ones. Also, SPEGA hydrogels showed higher modulus compared to other star PEG based hydrogels. The mass loss of the SPELA hydrogels initially increased with nL for up to 12 lactides per macromonomer, followed by a decrease which was attributed to the size of the micelles and reduced local water concentration. Also, SPEGA hydrogels showed fastest degradation rate among all kinds of hydrogel due to its less hydrophobicity and higher concentration of ester groups. MSCs encapsulated in BMP2-loaded SPELA hydrogel produced a mineralized matrix with up-regulation of osteogenic markers Dlx5, Runx2,

OP, and OC. Results demonstrate that hydrolytically-degradable PEG-based hydrogels is potentially useful as a delivery matrix for MSCs in tissue regeneration.

References

1. Moeinzadeh, S.; Barati, D.; He, X. Z.; Jabbari, E., Gelation Characteristics and Osteogenic Differentiation of Stromal Cells in Inert Hydrolytically Degradable Micellar Polyethylene Glycol Hydrogels. Biomacromolecules 2012, 13, (7), 2073-2086.

2. Moeinzadeh, S.; Khorasani, S. N.; Ma, J.; He, X.; Jabbari, E., Synthesis and gelation characteristics of photo-crosslinkable star Poly (ethylene oxide-co-lactide-glycolide acrylate) macromonomers. Polymer 2011.

3. He, X. Z.; Jabbari, E., Material properties and cytocompatibility of injectable MMP degradable poly(lactide ethylene oxide fumarate) hydrogel as a carrier for marrow stromal cells. Biomacromolecules 2007, 8, (3), 780-792.

4. Sarvestani, A. S.; Xu, W. J.; He, X. Z.; Jabbari, E., Gelation and degradation characteristics of in situ photo-crosslinked poly(L-lactid-co-ethylene oxide-co-fumarate) hydrogels. Polymer 2007, 48, (24), 7113-7120.

5. Sarvestani, A. S.; He, X. Z.; Jabbari, E., Viscoelastic characterization and modeling of gelation kinetics of injectable in situ cross-linkable poly(lactide-co-ethylene oxide-co-fumarate) hydrogels. Biomacromolecules 2007, 8, (2), 406-415.

6. Peppas, N.A., et al., Hydrogels in Biology and Medicine: From Molecular Principles to Bionanotechnology. Adv. Mater. 2006, 18, 1345–1360.

7. Serra, L., J. Domenech, and N.A. Peppas, Design of poly(ethylene glycol)-tethered copolymers as novel mucoadhesive drug delivery systems. European Journal of Pharmaceutics and Biopharmaceutics, 2006. 63(1): p. 11-18.

8. Simonsen, L., et al., Dextran hydrogels for colon-specific drug delivery. V. Degradation
in human intestinal incubation models. European Journal of Pharmaceutical Sciences, 1995. 3(6): p. 329-337.

9. Takamura, A., F. Ishii, and H. Hidaka, Drug release from poly(vinyl alcohol) gel prepared by freeze-thaw procedure. Journal of Controlled Release, 1992. 20(1): p. 21-27.

10. Chen, X., et al., Enzymatic and chemoenzymatic approaches to synthesis of sugar-based
polymer and hydrogels. Carbohydrate Polymers, 1995. 28(1): p. 15-21.

11. Gayet, J.C. and G. Fortier, High water content BSA-PEG hydrogel for controlled release
device: Evaluation of the drug release properties. Journal of Controlled Release, 1996. 38(2-3): p. 177-184.

12. Hubbell, J.A., Hydrogel systems for barriers and local drug delivery in the control of wound healing. Journal of Controlled Release, 1996. 39(2-3): p. 305-313.

13. Peppas, N.A. and J.J. Sahlin, Hydrogels as mucoadhesive and bioadhesive materials: a
review. Biomaterials, 1996. 17(16): p. 1553-1561.

14. Hoffman, A.S., Hydrogels for biomedical applications. Advanced Drug Delivery Reviews, 2002. 54(1): p. 3-12.

15. Lin, C.-C. and A.T. Metters, Hydrogels in controlled release formulations: Network design and mathematical modeling. Advanced Drug Delivery Reviews, 2006. 58(12-13): p. 1379-1408.

16. Peppas, N.A., et al., Hydrogels in pharmaceutical formulations. European Journal of Pharmaceutics and Biopharmaceutics, 2000. 50(1): p. 27-46.

17. Wichterle, O. and D. Lim, Hydrophilic Gels for Biological Use. Nature, 1960. 185(4706): p. 117-118.

18. Kim, B. and N.A. Peppas, In vitro release behavior and stability of insulin in complexation hydrogels as oral drug delivery carriers. International Journal of Pharmaceutics, 2003. 266(1-2): p. 29-37.

19. Ryu, J.-M., et al., Increased bioavailability of propranolol in rats by retaining thermally
gelling liquid suppositories in the rectum. Journal of Controlled Release, 1999. 59(2): p. 163-172.

20. Veronese, F.M., et al., Influence of PEGylation on the Release of Low and High Molecular-Weight Proteins from PVA Matrices. 1999. p. 315-330.

21. Ji, H., et al., Kinetics of thermally induced swelling of hydrogels. International Journal of
Solids and Structures, 2006. 43(7-8): p. 1878-1907.

22. Russell, R.J., et al., Mass transfer in rapidly photopolymerized poly(ethylene glycol)

hydrogels used for chemical sensing. Polymer, 2001. 42(11): p. 4893-4901.

23. Lee, S.-H. and H. Shin, Matrices and scaffolds for delivery of bioactive molecules in bone and cartilage tissue engineering. Advanced Drug Delivery Reviews. In Press, Corrected Proof.

24. De Laporte, L. and L.D. Shea, Matrices and scaffolds for DNA delivery in tissue engineering. Advanced Drug Delivery Reviews. In Press, Corrected Proof.

25. Yadavalli, V.K., et al., Microfabricated protein-containing poly(ethylene glycol) hydrogel arrays for biosensing. Sensors and Actuators B: Chemical, 2004. 97(2-3): p. 290-297.

26. Cohen, S., et al., A novel in situ-forming ophthalmic drug delivery system from alginates
undergoing gelation in the eye. Journal of Controlled Release, 1997. 44(2-3): p. 201-208.

27. Dolbow, J., E. Fried, and H. Ji, A numerical strategy for investigating the kinetic response of stimulus-responsive hydrogels. Computer Methods in Applied Mechanics and Engineering, 2005. 194(42-44): p. 4447-4480.

28. George, M. and T.E. Abraham, pH sensitive alginate-guar gum hydrogel for the controlled delivery of protein drugs. International Journal of Pharmaceutics, 2007. 335(1-2): p. 123-129.

29. Patel, V.R. and M.M. Amiji, Preparation and Characterization of Freeze-dried Chitosan-Poly(Ethylene Oxide) Hydrogels for Site-Specific Antibiotic Delivery in the Stomach. Pharmaceutical Research, 1996. 13(4): p. 588-593.

30. Achar, L. and N.A. Peppas, Preparation, characterization and mucoadhesive interactions of poly (methacrylic acid) copolymers with rat mucosa. Journal of Controlled Release, 1994. 31(3): p. 271-276.

31. Peppas, N.A. and A.R. Khare, Preparation, structure and diffusional behavior of hydrogels in controlled release. Advanced Drug Delivery Reviews, 1993. 11(1-2): p. 1-35.

32. Ajji, Z., I. Othman, and J.M. Rosiak, Production of hydrogel wound dressings using gamma radiation. Nuclear Instruments and Methods in Physics Research Section B: Beam Interactions with Materials and Atoms, 2005. 229(3-4): p. 375-380.

33. Ritger, P.L. and N.A. Peppas, A simple equation for description of solute release I. Fickian and non-fickian release from non-swellable devices in the form of slabs, spheres, cylinders or discs. Journal of Controlled Release, 1987. 5(1): p. 23-36.

34. Miyazaki, S., et al., Thermally reversible xyloglucan gels as vehicles for rectal drug

delivery. Journal of Controlled Release, 1998. 56(1-3): p. 75-83.

35. Fang, J.-Y., et al., Transdermal iontophoresis of sodium nonivamide acetate: V. Combined effect of physical enhancement methods. International Journal of Pharmaceutics, 2002. 235(1-2): p. 95-105.

36. Panza, J.L., et al., Treatment of rat pancreatic islets with reactive PEG. Biomaterials, 2000. 21(11): p. 1155-1164.

37. N.A. Peppas: Hydrogels in Medicine and Pharmacy, Vol. 1. Fundamentals, CRC Press,
Boca Raton, FL, 1986, 180 pages.

38. Malcolm B. Huglin, M.B.Z., Swelling properties of copolymeric hydrogels prepared by
gamma irradiation. 1986. p. 457-475

41. Amsden, B., Solute diffusion in hydrogels. An examination of the retardation effect. Polymer Gels and Networks, 1998. 6(1): p. 13-43.

42. Favre, E., et al., Diffusion of polyethyleneglycols in calcium alginate hydrogels. Colloids
and Surfaces A: Physicochemical and Engineering Aspects, 2001. 194(1-3): p. 197-206.
43. Flory, P.J., Molecular theory of rubber elasticity. Polymer, 1979. 20(11): p. 1317-1320.

44. Hickey, A.S. and N.A. Peppas, Mesh size and diffusive characteristics of semicrystalline
poly(vinyl alcohol) membranes prepared by freezing/thawing techniques. Journal of Membrane Science, 1995. 107(3): p. 229-237.

45. Lin, C.-C. and A.T. Metters, Hydrogels in controlled release formulations: Network design and mathematical modeling. Advanced Drug Delivery Reviews, 2006. 58(12-13):
p. 1379-1408.

46. Nikolaos A. Peppas, E.W.M., Crosslinked poly(vinyl alcohol) hydrogels as swollen elastic networks. 1977. p. 1763-1770.

47. Paul J. Flory, N.R.M.C.S., Dependence of elastic properties of vulcanized rubber on the
degree of cross linking. 1949. p. 225-245.

48. Peppas, N.A., et al., Hydrogels in pharmaceutical formulations. European Journal of Pharmaceutics and Biopharmaceutics, 2000. 50(1): p. 27-46.

49. Peppas, N.A., et al., Poly(ethylene glycol)-containing hydrogels in drug delivery. Journal

of Controlled Release, 1999. 62(1-2): p. 81-87.

50. Tiziana Canal, N.A.P., Correlation between mesh size and equilibrium degree of swelling of polymeric networks. 1989. p. 1183-1193.

51. Turner, A., Jr., The physics of rubber elasticity. L. R. G. Treloar, Oxford Univ. Press, New York, 1949, 262 pp. 1950. p. 387.

52 N.A. Peppas: Hydrogels in Medicine and Pharmacy, Vol. 1. Fundamentals, CRC Press,
Boca Raton, FL, 1986, 180 pages.

53 Hoffman, A.S., Hydrogels for biomedical applications. Advanced Drug Delivery Reviews, 2002. 54(1): p. 3-12.

54 Cruise, G.M., D.S. Scharp, and J.A. Hubbell, Characterization of permeability and network structure of interfacially photopolymerized poly(ethylene glycol) diacrylate hydrogels. Biomaterials, 1998. 19(14): p. 1287-1294.

55 Hennink, W.E. and C.F. van Nostrum, Novel crosslinking methods to design hydrogels.
Advanced Drug Delivery Reviews, 2002. 54(1): p. 13-36.

56 Lin, C.-C. and A.T. Metters, Hydrogels in controlled release formulations: Network design and mathematical modeling. Advanced Drug Delivery Reviews, 2006. 58(12-13): p. 1379-1408.

57 Mellott, M.B., K. Searcy, and M.V. Pishko, Release of protein from highly cross-linked
hydrogels of poly(ethylene glycol) diacrylate fabricated by UV polymerization. Biomaterials, 2001. 22(9): p. 929-941.

58 Merrill, E.W., K.A. Dennison, and C. Sung, Partitioning and diffusion of solutes in hydrogels of poly(ethylene oxide). Biomaterials, 1993. 14(15): p. 1117-1126.

59 Pathak, C.P., A.S. Sawhney, and J.A. Hubbell, Rapid photopolymerization of immunoprotective gels in contact with cells and tissue. 1992. p. 8311-8312.

60 Peppas, N.A., et al., Hydrogels in pharmaceutical formulations. European Journal of Pharmaceutics and Biopharmaceutics, 2000. 50(1): p. 27-46.

61 Peppas, N.A. and J.J. Sahlin, A simple equation for the description of solute release. III.
Coupling of diffusion and relaxation. International Journal of Pharmaceutics, 1989. 57(2): p. 169-172.

62 Perez, J.P.H., E. Lopez-Cabarcos, and B. Lopez-Ruiz, The application of methacrylatebased
polymers to enzyme biosensors. Biomolecular Engineering, 2006. 23(5): p. 233-245.

63 Ritger, P.L. and N.A. Peppas, A simple equation for description of solute release I. Fickian and non-fickian release from non-swellable devices in the form of slabs, spheres, cylinders or discs. Journal of Controlled Release, 1987. 5(1): p. 23-36.

64 Russell, R.J., et al., Mass transfer in rapidly photopolymerized poly(ethylene glycol) hydrogels used for chemical sensing. Polymer, 2001. 42(11): p. 4893-4901.

65 Park, H. and K. Park, Biocompatibility Issues of Implantable Drug Delivery Systems. Pharmaceutical Research, 1996. 13(12): p. 1770-1776.